LAWRENCE
LIVERMORE
NATIONAL
LABORATORY

UCRL-TR-208476

# Preliminary Evaluation of Techniques to Fabricate Beryllium, Polyimide, and Ge-doped CH/CD Ablator Materials

Bob Cook, Steve Letts, Abbas Nikroo, Art Nobile, Mike McElfresh, Jason Cooley, Dave Alexander

December 8, 2004

This work was performed under the auspices of the U.S. Department of Energy by University of California, Lawrence Livermore National Laboratory under Contract W-7405-Eng-48.

# Contents

## Introduction

The WBS4.2 capsule plan has as an FY04 IDI level 2 deliverable:

> IDI-4.2:1-04 Complete preliminary evaluation of techniques to fabricate beryllium, polyimide, and Ge-doped CH/CD ablator materials.

This report including appendices provides information to complete this deliverable. It summarizes the important features of each ablator material, with particular focus to its usefulness for ignition capsules. More detailed discussions of each ablator type are in the Appendix. Included at the end of each separate discussion in the Appendix is a list of all published work with an ICF focus on that ablator type.

This report is organized into Be based and polymer (C) based ablators. We summarize status, outstanding issues, and how we plan to address them. Details are in the Appendix. For Be there are two fabrication routes, one by machining bulk pieces into hemi-shells which are then bonded together, and the other by sputtering Be with Cu dopant onto spherical plastic mandrels to build up a wall. This method allows for radial variation in the Cu dopant concentration, while the machining approach is best suited to a uniform doping level. For plastic, we have already made a down select, eliminating polyimide because its performance as an ablator has been seen to be significantly different from that predicted by simulations. The other polymer, GDP (glow discharge polymer or sometimes called plasma polymer) comes in both a normal (hydrogenated) and deuterated form. There are differences between them (besides the H or D) and these will be detailed. The choice between them will be determined in part by cryogenic measurement of the IR absorption spectrum of DT scheduled to occur in the next few months.

An initial list of specifications for ignition targets exists. However these specifications are continuing to evolve. This is due to evolving plans for NIF's deliverable energy and to more refined design simulations. Many requirements are not well specified due to lack of knowledge of the effect on the implosion. These requirements include: grain size and texture, fill hole size, fill tube size, bond joint thickness, allowable porosity (size and number), diameter and wall thickness. Experiments are currently underway to assess the effect of grain size and texture, fill hole size, fill tube size, and bond joint thickness on the implosion. These parameters are being specified by simulation where possible. In cases such as bond joint thickness and fill hole size, the calculation methods are still under development. Completion of ignition capsule development will require final specifications.

## Beryllium Shells

## Status

### Sputtered shells

For sputtered shells we have demonstrated, though not perfected, the following:

- One Be sputter deposition of Cu-doped layers on 2 mm plastic mandrels. Sequential layers of 18 μm pure Be, 18 μm of 0.34 atom % Cu-doped Be, 27 μm of 0.65 atom % Cu-doped Be, 27 μm of 0.34 atom % Cu-doped Be, and ~15 μm of pure Be were deposited. Surface finishes at each layer were measured and were rougher than specifications. The grains are radially oriented, less than a micron in

diameter, and the Cu concentration is uniform (no build up or depletion at grain boundaries).

- The removal of the plastic mandrel through the laser drilled hole by pyrolysis.

- Material strengths in thin (~20 μm) shells approaching what is needed for room temperature handling of a full fill (~350 atm) in a full thickness NIF shell.

**Machined shells**

For machined shells the following processes have been demonstrated:

- Synthesis of bulk Be which is doped at the 0.9 atom % level with Cu by arc melting to limit the level of oxygen (and other impurities) in the material.

- Development of equal channel angular extrusion (ECAE) techniques to reduce grain size to 20-50 μm

- Machining techniques to produce matching hemi-shells that meet low mode (~8 and less) symmetry specifications. Higher mode specifications cannot be met by machining alone.

- Bonding techniques that result in bonds between the two hemis that are approaching the strength of the base metal.

**Sputtered and machined shells**

Some fabrication requirements such as filling and polishing are common to both beryllium fabrication methods. The following have been demonstrated:

- Polishing on flat Be substrates that shows the surface finish can be improved to a level similar to that need for NIF shells. No detailed polishing studies have been done on sputtered material, but in the process of looking at grain structure in sputtered material a flat surface was polished on a sputtered Be shell and no unusual effects were noticed.

- 3 μm holes have been laser drilled through 175 μm flat Be disks, and ~105 μm through a sputtered Be shell.

- Preliminary studies of laser sealing have been started.

- Initial aspects of fill tube fabrication and attachment have been started. 10 μm glass and plastic tubes have been fabricated. 10-12 μm diameter counter bores in a flat metal substrate using EDM techniques has been demonstrated.

The details of this work can be found in the Appendix.

## Issues

### Sputtered shells

- Sputter deposition must be optimized:

  a) The interfaces between layers reflect the surface roughness at this point in the deposition. Specifications for interface morphology at dopant layer interfaces must be established and the morphology controlled.
  b) We must increase the strength of the sputtered shells for the laser sealing - room temperature transport route to fielding.
  c) We must reduce or eliminate intergrain voids.

All three of these problems may respond to the same solution, namely densifying the sputtered material by various techniques, primary among them the use of ion bombardment during coating.

### Machined shells

- The most important issue here is the degree of grain refinement that can be accomplished. There is not yet a real specification, though an experimental program is in progress to study this issue. However final resolution is not expected until NIF shots are available. A focus for the next 2 years is establishment of the limiting grain size that can be achieved consistent with the rest of the process, particularly the thermally mediated bonding process.

- We must demonstrate with a newly installed precision lathe that capsules meeting low mode (<10) symmetry specifications can be routinely made. It is anticipated that significant improvements in low mode quality versus what was previously demonstrated will be achieved with the new lathe.

- Recent advances in bonding must be verified and optimized so that bonds with strengths similar to the base material can routinely be formed.

### Sputtered and machined shells

- The polishing capability that has been demonstrated on flats must be transferred to spheres. In addition we must make sure that processes that produce smooth surfaces at high modes do not destroy the low mode symmetry. There may be differences between sputtered and machined shells both with regard to method and efficacy of polishing.

- We have demonstrated laser drilling, but this must be made more routine and repeatable on full thickness shells.

- Laser sealing must be fully explored in FY05. It appears that machined and bonded shells will be strong enough to hold the fill at room temperature. The situation for sputtered shells is less clear. However even if sputtered shells are not strong enough, we must still develop laser sealing since it is the most direct route to low pressure gas fills for ambient temperature shots.

- Fill tube technology must be explored and developed. Even if the shells are strong enough for laser sealing it is not clear that this is the best way to field cryo ignition shots.

## Plans

### Sputtered shells

- We must understand how the sputter coating process effects the microstructure of the deposited material. Our focus will be on two parameters, the evolving surface finish and the material strength. The first is important for the quality of the interface between layers of different dopant concentration, and the strength is important for keeping room temperature handling of laser sealed filled shells an option. At LLNL there will be two coaters pursuing these efforts, and at GA's UCSD facility one coater. It is unclear at this time whether LANL will bring up a sputter coater. At LLNL the first effort (already in progress) will be to introduce an ion gun into the coating process in order to densify and potentially smooth the coating. GA has indicated they will look at shadowing mitigation approaches.

### Machined shells

- LANL will continue to work on the bonding to optimize it and make it reproducible. They will also continue the work on grain refinement. The extent to which low mode spherical quality of spheres can be improved with a new high precision lathe will be determined. Recent results have indicated that a finishing cut with a diamond tool on surfaces machined with cubic boron nitride can significantly improve surface finish. The extent to which a final cut with a diamond tool affects high mode surface quality on spheres will also be determined.

### Sputtered and machined shells

- One major activity will be in the area of polishing. Both LANL and GA will develop lap polishing techniques for shells, the focus for the end of the year being to see what surface finishes can be obtained without losing the low mode sphericity.

- GA and LANL will work on laser sealing approaches to filling. During the second half of FY05 GA intends to demonstrate the laser sealing of low pressure gas filled shells.

- LLNL will focus on fill tube attachment technologies, with a goal for the end of the year to demonstrate the attachment of a 10 μm fill tube to a Be capsule with a laser drilled hole.

## Plastic Shells

Although the polyimide program was very successful in meeting surface finish specifications, the choice of GDP over polyimide has already been made for two reasons. First, graded dopant capsules have superior implosion stability in simulations. However, polyimide, because of its levels of oxygen and nitrogen, does not allow (from a plasma physics point of view) for doping at all, much less gradient doping. Second, results from ablator physics (WBS3)

experiments on polyimide foils do not agree with simulations, in contrast to Ge- or Br-doped CH. The uncertainty surrounding polyimide as an ablator has led to the down-selection. The polyimide work has stopped and the process has been fully documented.

Work on GDP shells has shown that full thickness (undoped) CH shells can be produced meeting the NIF standard. Continued work on process improvement and control is needed to increase capsule yield. We have learned a great deal about what causes the full thickness shells to be out of specification, and progress is being made to remedy this situation. We have also shown that Ge doping gradients can be deposited. From many years of experience we expect that the addition of Ge-dopant in gradient layers will not significantly affect the surface finish.

In FY05 we expect to learn how to effectively control the low levels of doping that are required, and by the end of the year coat full thickness capsules with Ge-doped layers similar to that required in current designs. If cryo experiments indicate that deuterated coatings would provide better IR transmission at the wavelengths used, then two things will need to happen. First we will need to optimize deuterated coatings for smoothness. There are some minor differences between how CH and CD are deposited, but achieving NIF surface specifications should not be compromised by moving to deuterated coatings. We must also find a source of the dopant. Currently we are using tetramethyl germane in the flow gas. To produce a fully deuterated coating we will need to procure fully deuterated tetramethyl germane, and this will require custom synthesis. During this year General Atomics will explore this option.

Although plastic shells are diffusion fillable they are not strong enough to hold the full fill at room temperature. Thus we are exploring laser drilling and fill tube technologies.

# Appendix

Attached here are more detailed discussions of each ablator type. Following each discussion is a bibliography of published work (and in some cases internal LLNL documents). Although we have not reviewed mandrel technologies they are relevant for all capsules except machined Be. Thus we include a bibliography of papers related to mandrel production.

## Mandrel Bibliography


U. Kubo and H. Tsubakihara, *J. Vac. Sci. Technol. A* **4**, 1134 (1986).

M. Takagi, T. Norimatsu, T. Yamanaka, and S. Nakai, “Development of Deuterated Polystyrene Shell for Laser Fusion by Means of a Density-Matched Emulsion Method,” *J. Vac. Sci. Technol. A* **9**, 2145 (1991).

S. A. Letts, E. M. Fearon, S. R. Buckley, M. D. Saculla, L. M. Allison, and R. Cook, “Preparation of Hollow Shell ICF Targets Using a Depolymerizable Mandrel,” in *Mat. Res. Soc. Symp. Proc.* **372**, 125 (1995).

T. Boone, L. Cheung, D. Nelson, D. Soane, G. Wilemski, and R. Cook, “Modeling of Microencapsulated Polymer Shell Solidification,” in *Mat. Res. Soc. Symp. Proc.* **372**, 193 (1995).

G. Wilemski, T. Boone, L. Cheung, D. Nelson, and R. Cook, “Prediction of Phase Separation During the Drying of Polymer Shells,” *Fusion Technol.* **28**, 1773 (1995).

S. A. Letts, E. M. Fearon, S. R. Buckley, M. D. Saculla, L. M. Allison, and R. Cook, “Fabrication of Hollow Shell ICF Targets using a Depolymerizable Mandrel,” *Fusion Technol.* **28**, 1797 (1995).

S. A. Letts, E. M. Fearon, L. M. Allison, and R. Cook, “Fabrication of Special Inertial Confinement Fusion Targets Using a Depolymerizable Mandrel Technique,” *J. Vac. Sci. Technol. A* **14**, 1015 (1996).

B. W. McQuillan, A. Nikroo, D. A. Steinman, F. H. Elsner, D. G. Czechowicz, M. L. Hoppe, M. Sixtus, and W. J. Miller, "The PAMS/GDP Process for Production of ICF Target Mandrels," *Fus. Technol.* **31**, 381 (1997).

R. Cook, P. M. Gresho, and K. E. Hamilton “Examination of Some Droplet Deformation Forces Related to NIF Capsule Sphericity,” *J. Moscow Phys. Soc.* **8**, 221 (1998).

T. Norimatsu, Y. Izawa, K. Mima, and P. M. Gresho, "Modeling of the Centering Force in a Compound Emulsion to Make Uniform Plastic Shells for Laser Fusion Targets," *Fus. Technol.* **35**, 147 (1999).

P. M. Gresho, "Some Aspects of the Hydrodynamics of the Microencapsulation Route to NIF Mandrels," *Fus. Technol.* **35**, 157 (1999).

B. W. McQuillan and A. Greenwood, "Microencapsulation Process Factors which Influence the Sphericity of 1 MM OD Poly(alpha-methylstyrene) Shells for ICF. *Fus. Technol.* **35**, 194 (1999).

B. W. McQuillan, F. H. Elsner R. B. Stephens, and L. C. Brown, "The Use of $CaCl_2$ and Other Salts to Improve Surface Finish and Eliminate Vacuoles in ICF Microencapsulated Shells," *Fus. Technol*. **35**, 198 (1999).

R. Cook, S. R. Buckley, E. Fearon, and S. A. Letts “New Approaches to the Preparation of PαMS Beads as Mandrels for NIF-Scale Target Capsules,” *Fusion Technol.* **35**, 206 (1999).

M. Takagi, R. Cook, R. Stephens, J. Gibson, and S. Paguio, “Decreasing Out-of-Round in Poly(α-methylstyrene) Mandrels by Increasing Interfacial Tension,” *Fusion Technol.* **38**, 46 (2000).

M. Takagi, R. Cook, R. Stephens, J. Gibson, and S. Paguio, “Stiffening of PαMS Mandrels During Curing,” *Fusion Technol.* **38**, 50 (2000).

M. Takagi, R. Cook, R. Stephens, J. Gibson, and S. Paguio, “The Effects of Controlling Osmotic Pressure on a PαMS Microencapsulated Mandrel During Curing,” *Fusion Technol.* **38**, 54 (2000).

B. W. McQuillan and M. Takagi, "Removal of Mode 10 Surface Ripples in ICF/PAMS Shells," *Fus. Technol*. **41**, 209 (2002).

M. Takagi, R. Cook, B. McQuillan, F. Elsner, R. Stephens, A. Nikroo, J. Gibson and S. Paguio, “Development of High Quality Poly(α-methylstyrene) Mandrels for NIF,” *Fusion Sci. Technol.* **41**, 278 (2002).

A. Nikroo, J. Bousquet, B. W. McQuillan, R. Paguio, M. Takagi, and R. Cook, “Progress in 2 mm Glow Discharge Polymer Mandrel Development for NIF,” *Fusion Sci. Technol.* **45**, 165 (2004).

M. Takagi, R. Cook, B. W. McQuillan, J. Gibson, and S. Paguio, “Investigation of Larger Poly(α-methylstyrene) Mandrels for High Gain Designs Using Microencapsulation,” *Fusion Sci. Technol.* **45**, 171 (2004).

P. Subramanian, A. Zebib, and B. McQuillan, “Solutocapillary Convection in Spherical Shells,” accepted by *Physics of Fluids.*

## Cu-doped Sputtered Beryllium Capsules

### Introduction

Fabricating Be capsules using the physical vapor deposition (PVD) of Be metal requires a substrate (i.e. a spherical mandrel) as a template onto which the metal is deposited. Two commonly used PVD methods are evaporation and sputtering. For sputtering a small pressure of gas (in our case Ar) in the deposition chamber is used to generate a plasma at the surface of the sputter source. Collisions of the ionized gas atoms with the sputter source's target material cause target atoms to be ejected from the target surface and deposit onto the substrate. Applying a voltage bias between the substrate and the source can accelerate the atoms toward the substrate. While sputter sources are more limited in the rate that metal that can be deposited, a sputter source can be oriented in any direction providing more flexibility in the relative orientation of source and sample.

Uniform coverage of the metal over a sphere requires frequently reorienting the sample under the sputter source. Currently we keep the mandrel in constant motion using a bounce pan centered under the sputter sources thereby providing a nearly random reorientation. It is thought that during bouncing that there is a preference for the more massive side of the sphere to be oriented down allowing the lighter side facing up to be coated preferentially.

The currently desired capsule design is shown in Figure 1. It requires different bands of Cu-doped Be radially oriented. This can be accomplished by controlling the sputtering power to a Cu source as described below. An extensive memo describing our first graded Cu-doped Be deposition has been released and is listed first in the list of internal LLNL documents at the end of this section.

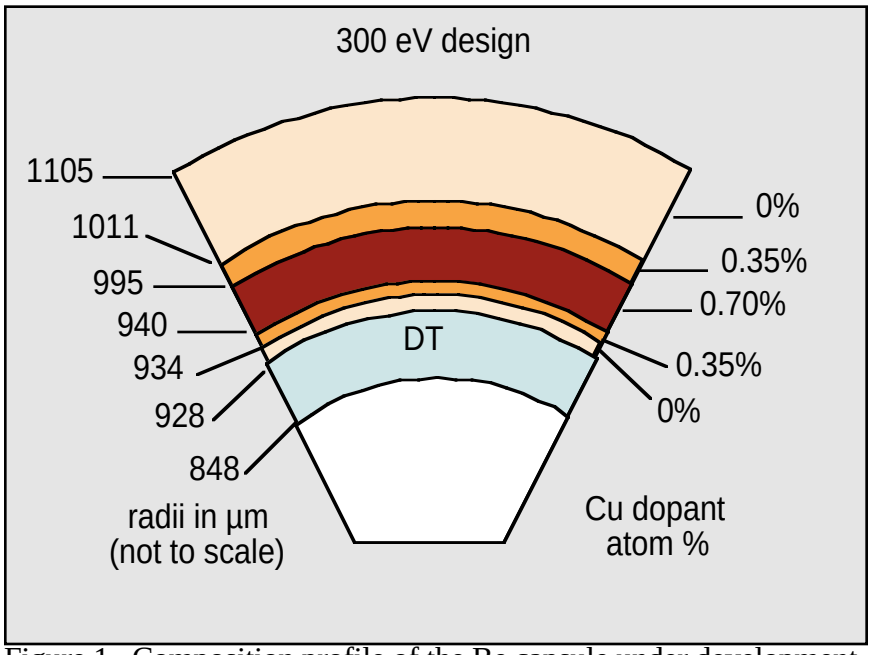

Figure 1. Composition profile of the Be capsule under development.

### Fabrication of Graded Cu-doped Be Capsules

To fabricate Cu-doped Be capsules we are using four Be sputter sources arranged on a square with a single Cu sputter source centered between the Be sources as shown in Figure 2.

Initially the 2 mm GDP mandrels are coated with a thin layer (i.e. 0.5 μm) of Be using a bounce pan that constrains their motion to a few millimeters and keeps capsules from touching each other. Once precoated, the capsules are less likely to stick together and precoated batches can be combined into a bounce pan where they can bounce a few millimeters off of the surface of the pan and move a maximum of about1 cm laterally.

The sputter sources are MAC brand; 2 inch guns for the Be and a 1 inch gun for the Cu. Because the Cu doping level is so small, an additional aperture is used to help reduce Cu flux and still allow the gun to be operated in a stable regime. The Be guns are operated at a level of 300 watts each while the Cu gun typically operates from 4 to 16 watts depending on the desired Cu doping level. An 80-volt bias is used during deposition and a 3.7 mTorr Ar atmosphere is maintained. Preliminary results suggest that the temperature on the bounce pan is about 250 °C during deposition.

Sputtering conditions can have a significant effect on the properties of the material produced. To obtain epitaxial single crystal films the substrate is kept at elevated temperatures (usually greater than 500 °C) and the substrate and film must have a good lattice match. For our Be capsules the GDP mandrel is not thermally stable at those temperatures and GDP does not provide any lattice matching. Significant differences are observed when Be films are prepared on flat substrates versus the spherical mandrels. In both cases the material grows with a columnar structure with grains perpendicular to the surface, however in the case of the 2 mm sphere the region between grains is low in density as observed using transmission electron microscopy (TEM) as shown in Figure 3. Low grain boundary densities are often associated with limited surface mobility of atoms on the substrate surface. This can be improved by increasing the surface temperature or the energy of the atoms hitting the surface. The voltage bias is a way to increase the energy of impinging atoms. Sputtered atoms also lose energy to collisions with the sputter gas so that a lower pressure in the deposition chamber favors a higher impinging-atom energy. An 80 volt bias improves the surface finish of the Be capsules, however we have not yet determined if the microstructure (i.e. grain boundary density) is affected. We are incorporating an ion source into the deposition system that will be used to add energy to the substrate surface with the intention of increasing surface mobility and thereby increasing the grain boundary density.

Figure 4 is a scanning electron micrograph cross section of a step graded Cu-doped Be sphere fabricated by sputtering during approximately 95 hours. The compositions of layers are close to the targeted values of 0, 0.35, and 0.7 atomic percent as determined by both neutron activation analysis and electron probe. The sputter guns were shut down every night and as each composition layer was completed the chamber was opened to remove a few capsules for study of the intermediate stages of fabrication. Even though the system is pumped to about $10^{-8}$ Torr when the sputter sources are off, Be oxides form as shown by the lighter lines in Figure 4. In addition, during the fabrication of these capsules the Cu-sputter source was at its full operating power as the Be sources were ramped each morning over tens of minutes to their full power. This procedure was originally instituted because some capsules were shown to deform if exposed to full sputter power too rapidly. This, however, results in regions of higher-than-targeted copper concentrations forming during the ramp period. Recently we have shown that we can eliminate the precoat stage for 2 mm GDP capsules and that after a few microns of pure Be have been deposited we can bring the power up quickly thereby eliminating the excursions in Cu concentration. We have also shown that we can run continuously and expect that this will greatly reduce or eliminate the formation of Be oxide layers.

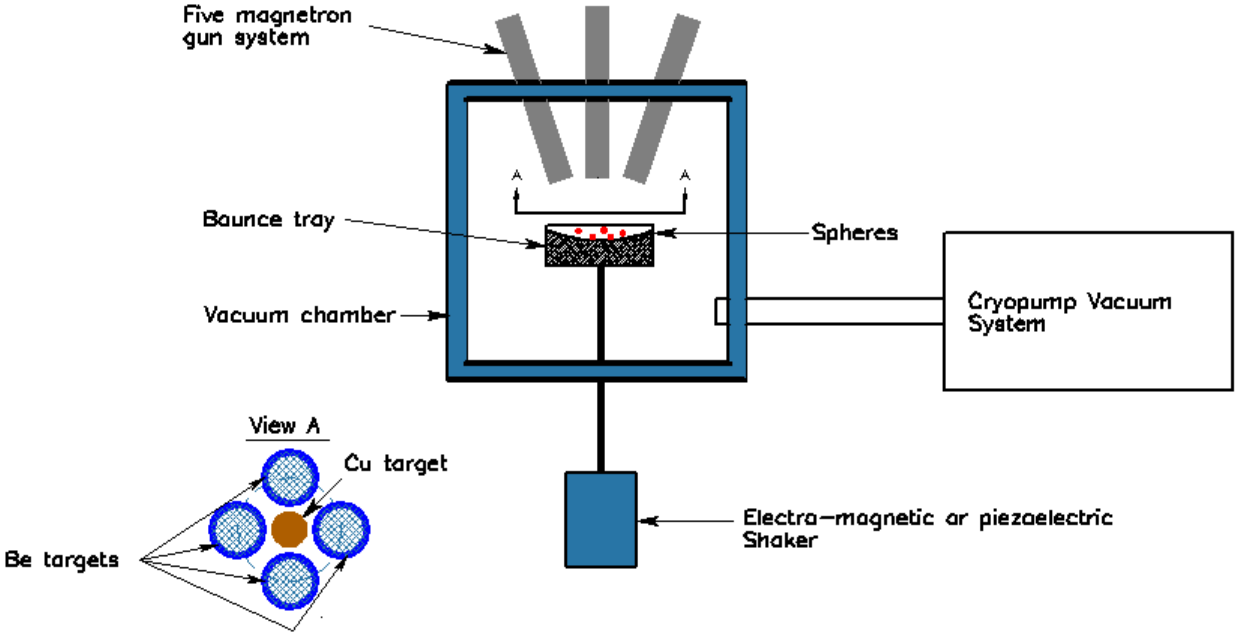


Figure 2. Schematic diagram of the Be sputter system. Four MAC 2-inch sputter guns arranged on a square are used to sputter the pure Be, while a single 1.3-inch MAC gun is used to sputter Cu. A piezoelectric driver is used to drive the pan in order to keep the capsules in motion.

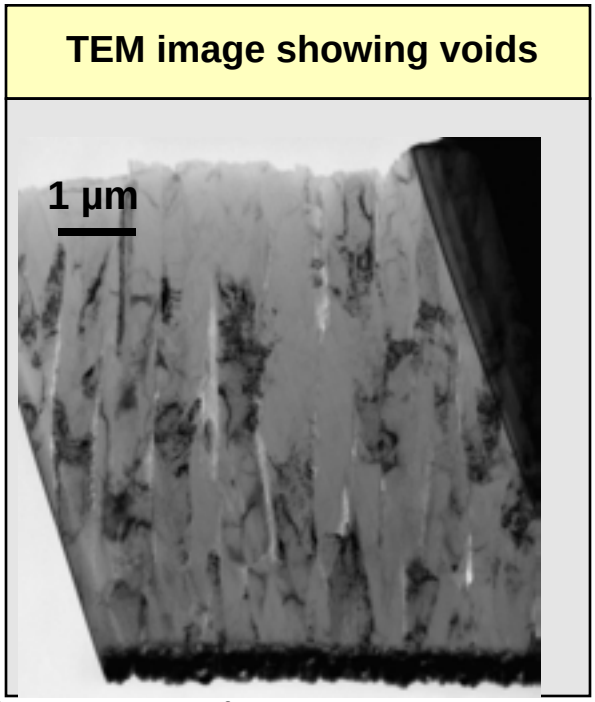


Figure 3. TEM of a FIB'ed sample form a coating on a 2 mm sphere. (Photo from work of Robert D. Field, LANL)

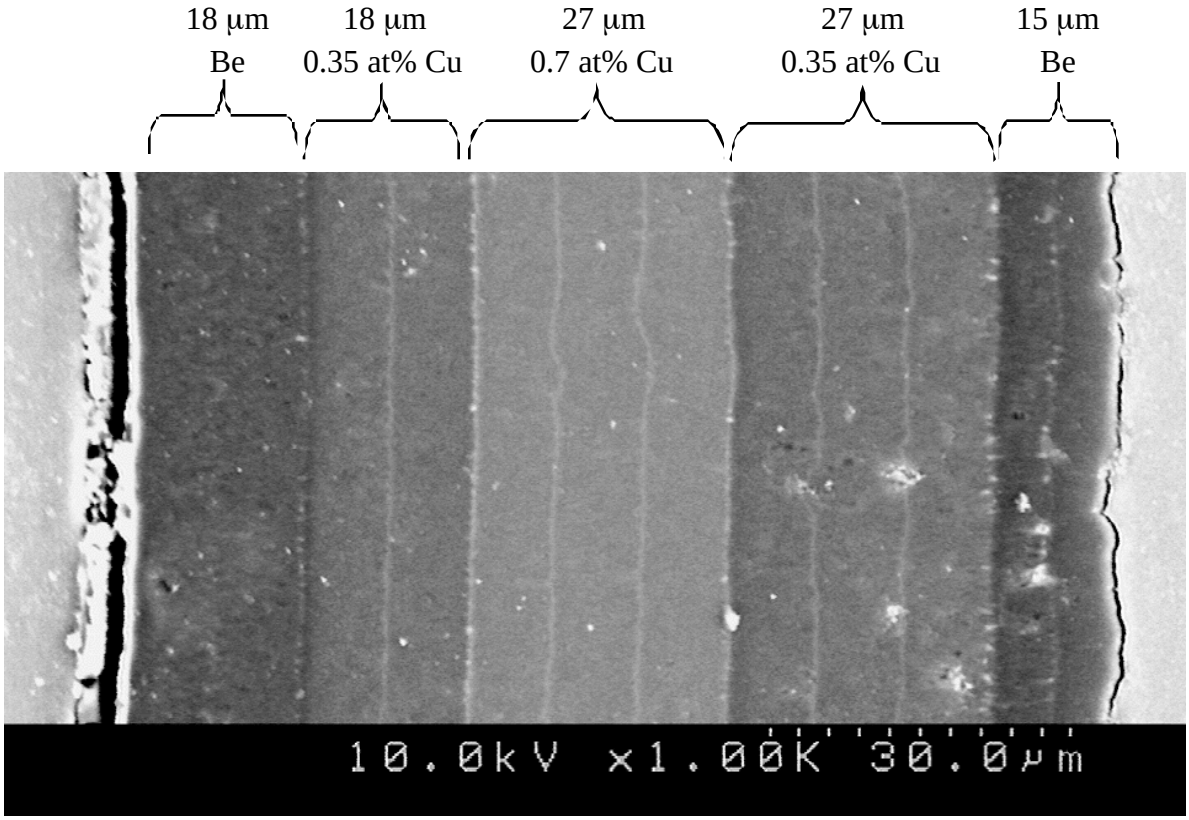


Figure 4. An SEM image of the polished cross-section of a step-graded Cu-doped be capsule prepared by sputtering. The change in brightness reflects the differences in Cu doping level. The brightest lines (nearly white) occur approximately every 8-9 μm and represent the interface between daily runs. Analysis with EDS suggested increased oxygen content in these thin regions.

Shown in Figure 5 are successive power spectras of shells removed after each Cu concentration level. The surface becomes rougher with thickness, a situation that can also be seen in Figure 4. Build-up of debris in the bouncer pan contributed to this roughness, in fact the run had to be terminated due to irreversible sticking problems related to the debris build up. We expect that this increasing roughness can be reduced partly by improved debris control, and partly as a side benefit of techniques to improve the grain packing such as the introduction of the ion gun. The growing roughness of the surface is clearly mirrored at the interfaces between layers, and this is a problem that must be addressed. We expect to improve the surface finish of the outside of the capsule by polishing. Previous work on flat substrates has shown that the power spectra can be brought below the current design specification for graded capsules. In FY05 GA and LANL will have vigorous programs to transfer these results from flats to spheres. A major concern is that the high mode surface finish not be improved at the cost of the low mode symmetry.

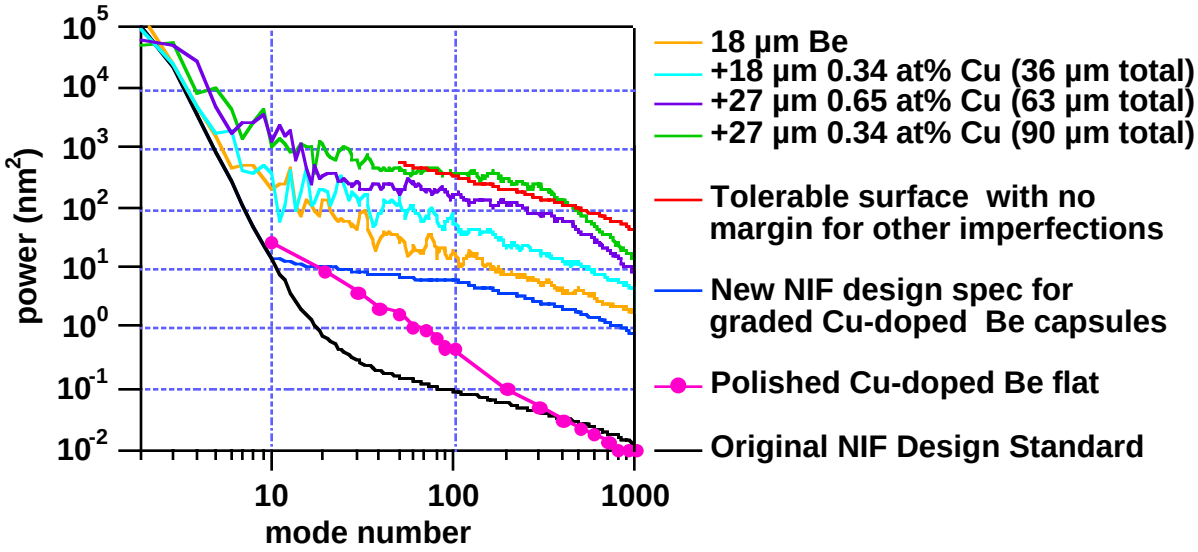


Figure 5. Successive power spectra of capsules taken from the coater after each Cu-doped layer.

**Fielding**

We have laser drilled a 2-3 μm fill hole through 175 μm of Be (as a flat substrate) and ~105 μm through a capsule wall (the thickest capsule we have to date). This capability is needed for two reasons. First, we must remove the inner plastic mandrel since at cryo temperatures the plastic shrinks more than the Be, leading to delamination from the inner Be wall. We have removed the plastic by pyrolyzing it at elevated temperatures while pumping air in an out of the shell through the small hole by varying the external pressure. An example of this removal is shown in Figure 6. On the left is a 20 μm thick Be shell deposited on a 14 μm thick plastic mandrel. A ~5 μm hole was drilled in this capsule and then it was subjected in a furnace to 450 °C air whose pressure was cycled between 1 and 5 atm over a period of about 1 min. This treatment continued for 35 hr. The result is shown by the radiograph on the right, showing that the plastic mandrel has been removed. In FY05 we will optimize this process.

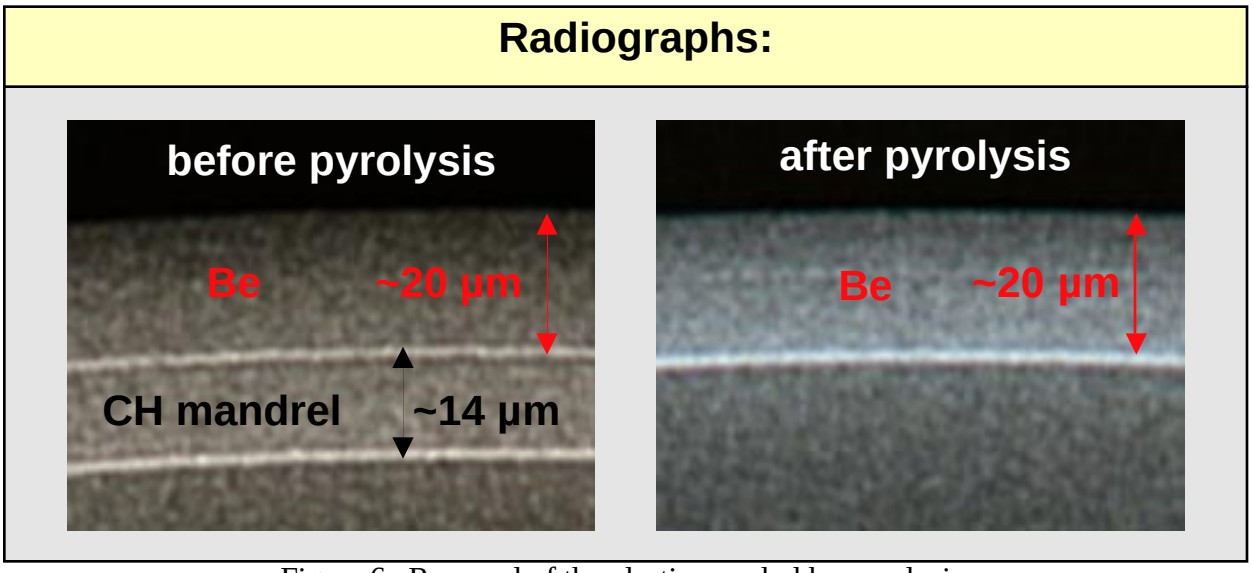


Figure 6. Removal of the plastic mandrel by pyrolysis.

The other important purpose of the drilled hole is filling. Be shells cannot be filled by diffusion, even at high temperatures, due to a impermeable thin oxide layer that forms on the surface. Thus we will either fill through the fill hole and then laser seal the hole, or develop fill tube technology and fill the capsule cold. A key requirement for the laser-sealing route is that the capsule be strong enough to hold the fill (~350 atm) at ambient temperatures. To measure the burst strength we have introduced water into the capsule through the drilled fill hole, and then sealed the hole with an excess of epoxy. The capsule is then placed in a chamber and the temperature slowly raised. The internal pressure is equal to the water vapor pressure, which is a function of temperature. The temperature (and thus the pressure) at which the capsule bursts is recorded. In Figure 7 we show typical results presented in terms of the % of bulk Be strength. The required strength of the graded Cu design with a safety factor of 2 is about 60% of the bulk Be strength.[1] The measured strength at the elevated burst temperature is about 45% of the bulk strength, but when extrapolated to ambient temperature it is about 65%. This extrapolation is based on data for bulk Be, and may not be quantitatively appropriate to sputtered Be on capsules. However the measured burst strength is at least close to that required. In FY05 we will change our method of measuring strength so that temperature extrapolation is not required. At the same time we need to work to improve strength, and we feel that the best approach is to increase grain packing as described above.

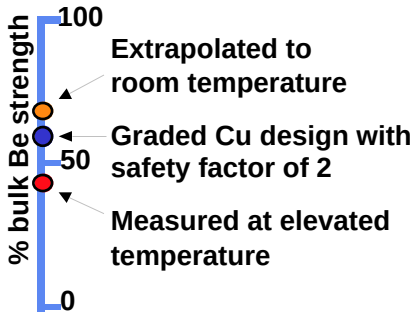


Figure 7. Strength measurement data for sputtered shells.

Initial hole sealing experiments by laser welding have yielded mixed results. We have demonstrated that Be can be melted by intense lasers, and have developed a thermal model that has been experimentally verified. Initial sealing experiments on Ni foil showed complete hole closure. Experiments on Be foil also showed hole closure, but also subsequent cracking of the material. However these results are too limited to draw any conclusions, and we anticipate a vigorous experimental program in FY05.

The other approach to filling if the capsules do not have sufficient strength to make laser sealing viable is to develop fill tube technology. This is certainly going to be necessary for plastic capsules, the differences for Be capsules may or may not be significant. In FY05 we will develop and test strategies.

## Reference

1. The value assumed for Be yield strength was 42.5 ksi (293 MPa), which is an average value for the ranges specified in the literature, see J. M. Marder, *J. Materials for Energy Systems* **8,** 17 (1986).

## Sputtered beryllium bibliography

R. McEachern, C. Alford, R. Cook, D. Makowiecki, and R. Wallace, “Sputter-Deposited Be Ablators for NIF Target Capsules,” *Fusion Technol.* **31**, 435 (1997).

A. K. Burnham, C. S. Alford, D. M. Makowiecki, T. R. Dittrich, R. J. Wallace, E. C. Honea, C. M. King, and D. Steinman, "Evaluation of $B_4C$ as an Ablator Material for NIF Capsules," *Fus. Technol*. **31**, 456 (1997).

R. McEachern and C. Alford, "Evaluation of Boron-doped Beryllium as an Ablator for NIF Target Capsules," *Fus. Technol*. **35,** 115 (1999).

R. Cook, M. Anthamatten, J. P. Armstrong, S. A. Letts, R. L. McEachern, B. W. McQuillan, and M. Takagi, “Recent Progress in the Development of Capsule Targets for the National Ignition Facility,” *Proc. of the SPIE* **5228**, 692 (2003).

The following are internal LLNL documents (in reverse chronological order)

J. Gunther, M. McElfresh, C. Alford, H. Huang, and B. Cook, "Fabrication and Characterization of Graded Cu-doped Be Shells - Details and Documentation of Our First Attempt," October 12, 2004, UCRL-TR-207361

B. Cook, "Hole Drilling Breakthrough Detection in Be Shells," September 17, 2004, UCRL-TR-207164.

B. Cook and J. Gunther, "Oxidation of Be at Elevated Temperature," September 16, 2004, UCRL-TR-207163.

B. Cook, S. Letts, and S. Buckley, "Experimental Confirmation of CH Mandrel Removal from Be Shells," June 8, 2004, UCRL-TR-204747.

B. Cook, "Measurement of Cu-doped Be Gradient Steps in Sputtered Be Capsules," March 26, 2004, UCRL-TR-203445

B. Cook, “Mandrel Burn-Out in Be Shells - Gas Flows,” March 9, 2004.

R. McEachern, "Argon Content of Sputter-Coated Be Shells," February 27, 2004.

B. Cook, “Mandrel Burn-Out in Be Shells,” October 28, 2003.

B. Cook, "Surface Perturbation Caused by Melt Sealing Drilled Be Capsules," November 20, 2002.

B. Cook, "Radiographic Characterization of Drilled (and Sealed) Holes," November 4, 2002.

B. Cook, "Sputtered Be Shell Strength Testing," January 31, 2002.

# Cu-doped Machined Beryllium Capsules

**Abstract**

Cu-doped Be capsules are being developed for experiments at the National Ignition Facility (NIF). Current LANL focus is based on fabrication by bonding of cylindrical parts containing precision machined hemispherical cavities, followed by machining an external spherical contour to produce a spherical shell. This approach to fabricating capsules has been demonstrated, but there are several key issues that need to be resolved before a shell meeting NIF specifications can be produced. This document describes the status of the development effort to produce capsule meeting NIF ignition specifications using this method. Also described are the milestones that must be achieved in order to produce capsule meeting ignition specifications.

## I. Introduction

The precision machining approach to fabricating a NIF ignition capsule is illustrated in Figure 1.

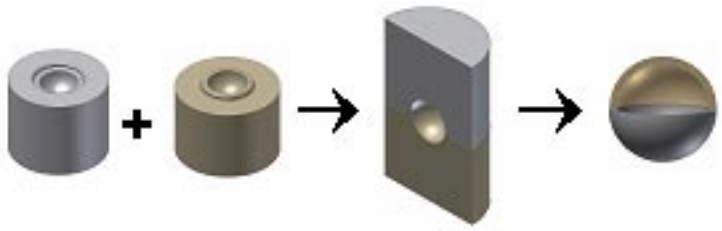

Figure 1. Precision machining approach to fabricating Be0.9%Cu capsule.

Fabrication begins with bulk Be0.9%Cu alloy cylinders that have a hemispherical cavity machined into them. These cylinders are bonded together in a special bonding process. The bonded cylinders are then precision machined to produce the hollow sphere. Figure 2 shows a radiograph and photograph of a 2 mm Be shell produced in this manner. The finished capsule is filled with DT either by cryo-condensation of DT through a small laser drilled hole followed by laser sealing the hole, or by attachment of a fill tube that fills the capsule in the NIF target positioner and remains attached to the capsule during the shot.

Present efforts are aimed at resolving issues that will allow capsules to be produced that meet the stringent ignition specifications (1,2). These issues are as follows:

- Synthesis of fine grain (<10 μm) full density isotropic high purity Be0.9%Cu alloy.
- Formation of a strong hemishell bond capable of containing fill gas at room temperature (with factor of 2 safety).
- Precision machining and final capsule polishing to meet ignition capsule shape specifications.
- DT filling.
- Development of characterization capabilities.

In this document we discuss the status of the above issues and the development plans that are aimed at producing a capsule that meets NIF ignition specifications.

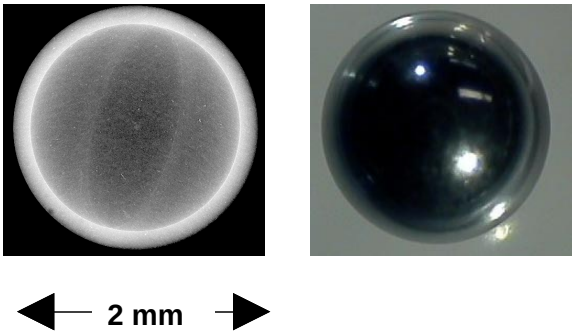


Figure 2. Radiograph and photograph of 2 mm diameter Be capsule with 150 μm wall.

## II. Synthesis of fine grain full density isotropic high purity Be0.9%Cu alloy

A requirement is to develop full density isotropic high purity Be-Cu alloy. The size specification for the grains is still unknown and is being determined by experimental and theoretical modeling work. It is estimated that this specification will require grains of <10 μm, so this is the current goal of the alloy production effort. Grain size must also be small relative to the capsule wall thickness (150 μm) so that the wall will have the strength characteristics of a polycrystalline material. Physics requirements dictate that impurities in the alloy must be less than $100\%/Z^2$, where Z is the atomic number of the impurity element. It is also important that the x-ray opacity of the alloy not vary by more than about 1 part in $10^4$ over length scales of ~50 μm. This requires very uniform dopant and impurity concentrations.

Fine grain Be and Be alloys are traditionally synthesized by hot isostatic powder pressing. While this produces fine grains, the metal inherently has oxygen concentrated at its grain boundaries from BeO on the surfaces of starting powder grains. Oxygen content in Be or Be alloy produced by this method is relatively high. For this reason, a synthesis scheme based on the powder pressing route was not chosen. The route chosen to produce alloy was by vacuum arc melting and subsequent grain refinement. Arc melting allows the alloy to be repeatedly melted and acid etched, which significantly reduces oxygen and other impurity content. Repeated melting of the alloy also ensures homogeneity of the dopant element. After repeated melting and etching of the alloy, it is vacuum drawn in a specially designed hearth to produce a rod.

Alloy produced by arc melting has relatively large and non-randomly oriented grains. Figure 3 shows the microstructure in transverse and longitudinal directions of a cast Be0.9%Cu alloy rod. These photos indicate that the grains are approximately cylindrical in shape and run in the radial direction. This microstructure has unacceptably large grains so the alloy must be grain refined. The process for grain refinement is by equal channel angular extrusion (ECAE). ECAE involves forcing the alloy through a channel as shown in Figure 4a. This process subjects the alloy to a high degree of strain, which results in grain refinement. Figure 4b shows sectioned samples of Be0.9%Cu alloy contained in Ni cans. Details on the ECAE grain refinement of Be and Be-Cu alloys are described in other publications (3,4).

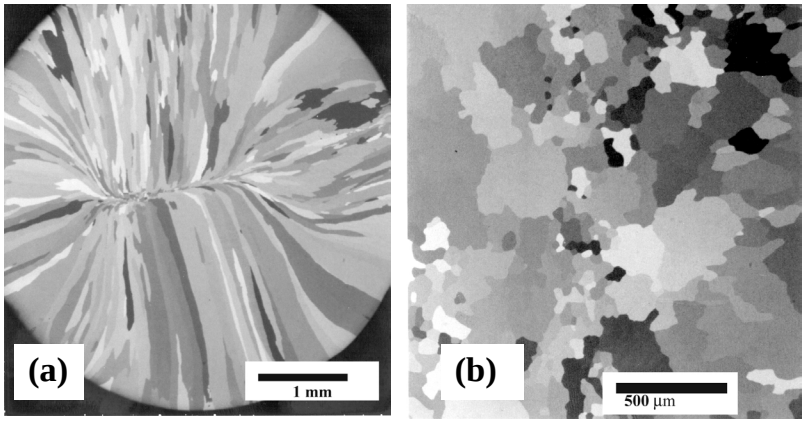


Figure 3. Microstructure of an as-cast Be0.9%Cu alloy rod; (a) transverse cross section and (b) longitudinal cross section.

The goal of the current effort is to determine the optimum grain refinement parameters (temperatures and method for passing the sample through the channel) that produce a fine grain microstructure with minimal texture. Figure 5 shows the microstructure of a Be0.9%Cu alloy with starting microstructure shown in Figure 3 that has been passed through the ECAE channel 4 times at 700 °C followed by a 775 °C 1 h anneal. Grain size has been significantly reduced, and grains are in the size range 20-50 μm. Optical and SEM examination of the alloy indicate that it is single phase and does not contain undesired oxide or other phases. Further characterization will reveal the extent of texture in this sample. Experimental and modeling efforts are underway to establish optimum grain refinement parameters that produce a fine grain low texture alloy. Current plans are to complete optimization of the grain refinement process by the end of FY06. At this time the extent of grain refinement that can be accomplished by the ECAE process will be known.

Elemental analysis of alloy produced by the above method has been partially completed. Of the elements in the periodic table, it will be necessary to analyze for 76 elements. To date, analysis has been performed for 13 elements. Of these elements, none have been found to be at levels above the $100\%/Z^2$ specification. Analysis was conducted on two alloy samples. Cu concentrations in these samples were prepared to be 6.0 wt%, but the analysis result was 6.7 and 4.7 wt%. Why the Cu concentrations were different and were not the expected 6.0 wt% is uncertain and will be the subject of future work.

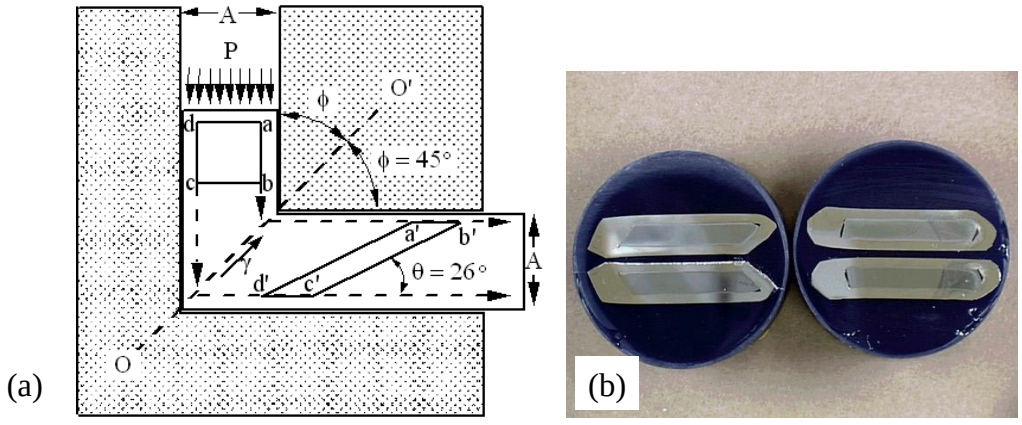


Figure 4. (a) ECAE process for grain refinement. (b) Sectioned Be0.9%Cu samples in nickel cans after ECAE processing.

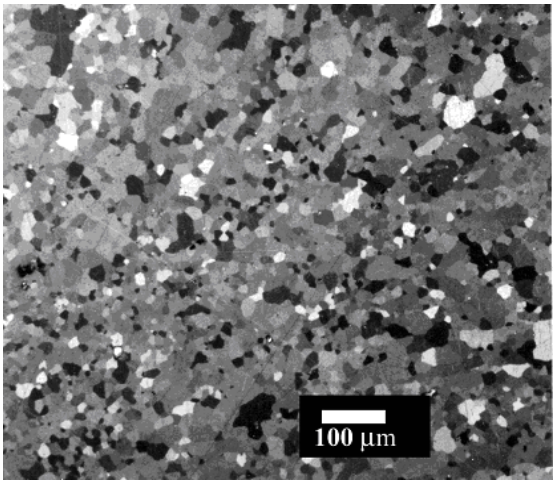


Figure 5. Microstructure of ECAE processed Be0.9%Cu alloy.

## III. Forming strong hemishell bonds capable of holding fill gas at room temperature

An important objective of the Be0.9%Cu capsule development effort is to develop capsules that are capable of holding their room temperature fill pressure (~400 atm). Depending on the particular ignition capsule design, a DT filled capsule at room temperature has a wall stress in the range 25-50% pure Be yield strength. Assuming a safety factor of 2 will be required, room temperature transport would be feasible if bonds can be developed with 50-100% of Be yield strength. Achieving this will allow capsules to be filled at a tritium facility, laser sealed and transported warm to NIF. Such an approach has advantages with respect to simplifying target fielding and eliminating the fill tube perturbation.

To accomplish room temperature transportability, we are working to establish a process for forming high strength bonds. The bonding process involves the use of a thin (<1 μm) metal layer that is deposited onto the bonding surfaces. This thin metal layer acts as a "glue" to hold the parts together. Previous experience with other larger Be geometries indicates that bonds with strengths near the strength of the bulk material have been formed.

The bonding process begins with sputter cleaning of the mating surfaces to remove native BeO present on air-exposed surfaces. In the same chamber a 0.7 μm Al layer is then deposited without air exposure. The parts are removed from the vacuum chamber, placed in another vacuum chamber where they are pressed together at high temperature to form the bond. Studies have been conducted to understand the sputter cleaning and Al deposition process and to verify that BeO is being eliminated before Al deposition. The results of these studies are documented elsewhere (5).

Table 1 summarizes the results of the bonding tests to date. The strongest bonds were formed at temperatures of 750 and 850 °C. In one test conducted at 750 °C, one of the bond mating surfaces was machined with a diamond tool to produce a smoother mating surface (due to tool clearance limitations, the female surface could not be diamond turned and was machined with a cBN tool). During burst testing of this part, the system pressure reached its pressure limit and the part did not burst. Thus the bond strength value in Table 1 represents a minimum value. The actual bond strength would likely be higher. The value assumed for Be yield strength was 42.5 ksi (293 MPa), which is an average value for the ranges specified in the literature.(6)

Table 1. Summary of results to date on Be-Be bond strength

| Bonding Temperature (°C) | % Be Yield Strength | Bond Conditions (all bonds formed for time of 600 s) |
|---|---|---|
| 700 | 19.7 | Bond mating surface machined with CBN tool, bond formed in vacuum. |
| 750 | 17.3 | Bond mating surface machined with CBN tool, bond formed in 6%$H_2$/He. |
| 750 | >74.3* | Male mating surface machined with diamond tool, female with CBN. Bond formed in vacuum. |
| 750 | 1.9 | Nitrides observed in bond by TEM examination. Air leak detected in Al coating chamber. |
| 750 | 44.8 | Bond mating surface machined with CBN tool, bond formed in vacuum. Bond was misaligned. |
| 850 | >71.4* | Bond mating surface machined with CBN tool, bond formed in vacuum. |

*These bonds could not be burst with the available gas pressure and these strengths represent the strength at the maximum pressure achieved in the test. Actual burst pressures would be higher.

In a bond formed at 700 °C in vacuum with cBN turned mating surfaces the strength was relatively low (19.7% Be yield strength), whereas another bond formed at 850 °C with cBN turned surfaces had relatively high strength (>71.4% Be yield strength). From this we conclude that with cBN turned mating surfaces, a strong bond cannot be formed at 700 °C, but strong bonds can be formed at higher temperatures. The bond formed at 750 °C that had its male mating surface diamond turned had relatively high strength. In a part bonded at the same temperature that had both mating surfaces machined with cBN the strength was significantly weaker (44.8% Be yield strength). However, this bonding part showed visible misalignment, so the results so far are inconclusive as to whether or not a smooth surface on one of the bonding parts produced higher bond strength.

Figure 6 plots the bond strength as a function of temperature. Strength above 50% of the bulk Be yield strength is needed for room temperature transport of currently known ignition designs. Factored into this strength is a safety factor of 2. From the results in Table 1 and Figure 6 we conclude that bonds can now be made with strengths sufficient for room temperature transport of some ignition capsule designs.

Current efforts are aimed at determining with higher certainty the level of bond strength that can be formed. As was mentioned above, bonds with high strengths could not be burst with the current burst system. In bonding tests now underway, the capsule wall thickness has been reduced to a thickness that can be burst in the high pressure burst test system. In these tests multiple bonds (approximately 3) will be formed at temperatures of 750 and 850 °C. In these tests the bonding parts have been modified so that both the male and female mating surfaces can be diamond turned and will have high quality surface finish. While the above results are inconclusive as to whether mating surfaces with lower roughness give higher bond strength, it is our intuition that this will be the case, so the next series of tests will involve mating surfaces that are diamond-machined.

In bond samples that could not be burst with the gas burst system, these bonds were broken by physically deforming the bond. This was done to verify that the gas fill tube was not plugged, and to observe the mode of bond failure. In both cases where the capsule could not be burst, it was verified that the fill tube was not plugged. Photographs of the bond failure surface were taken. Figure 7 shows the failure surface of one of these bonds. The bond has failed in the base Be

material and not along the bondline. This is encouraging since it suggests that the bond strength is approximately equal to or greater than the strength of the bulk Be material. The goal for FY05 work is to demonstrate the ability to form repeatable bonds with strengths that are 96% of beryllium yield strength.

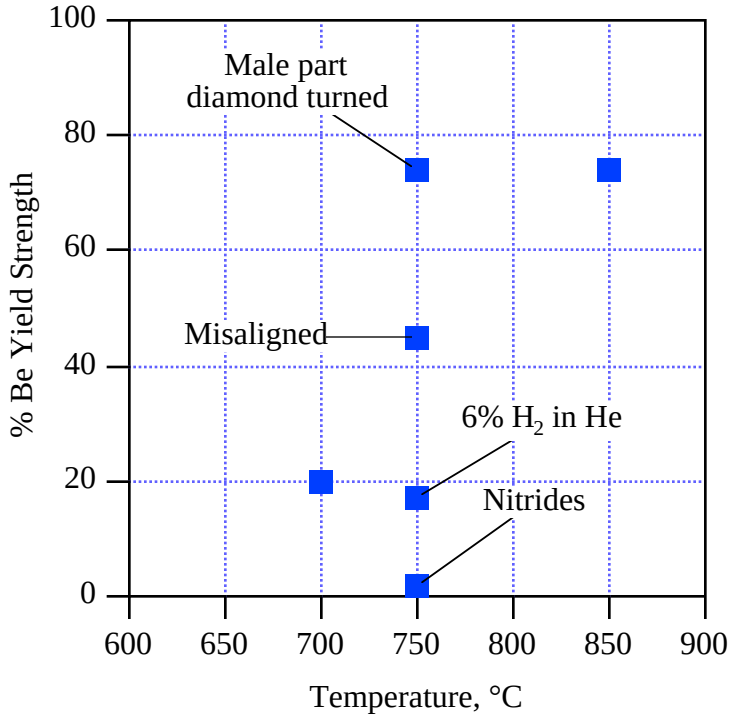


Figure 6. Summary plot of Be-Be bond strengths obtained to date. Strength above 50% of the bulk Be yield strength is needed for room temperature transport of currently known ignition designs, assuming a pressure containment safety factor of 2.

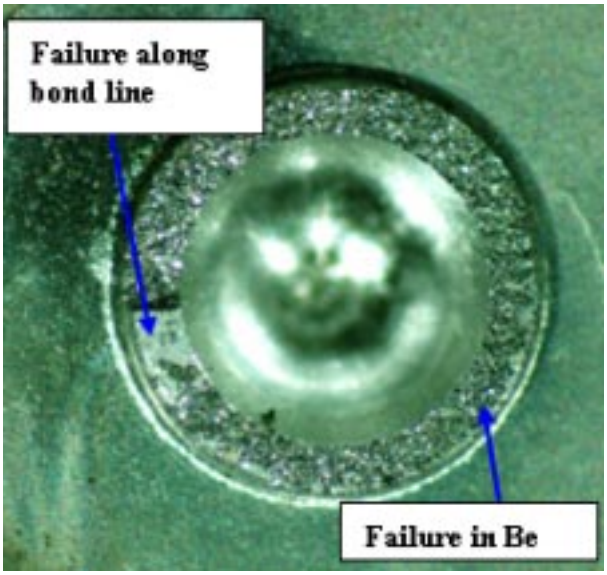


Figure 7. Optical photograph of failure of a Be-Be bond. Approximately 80% of the bond failed in the beryllium metal, indicating that most of the bond was as strong or stronger than the beryllium metal.

## IV. Precision machining and final polishing to meet ignition capsule shape specifications

Figure 8 shows the power spectrum results of a machined and polished capsule. This capsule was machined on an old diamond turning machine with a cBN tool and was polished in a ring lap polisher with unoptimized polishing compound. In addition to the traditional NIF standard curve, curves are shown in Figure 8 that represent new power spectrum standards for Be0.9%Cu capsules with uniform radial dopant. The curve labeled "No Margin" represents the required power spectrum for a capsule where surface roughness features are the only imperfections. The curve labeled "Margin" represents the required power spectrum where other imperfections exist in the target. This latter curve represents the capsule surface quality that should be achieved for ignition capsules. The data in Figure 8 indicate that low mode shape specifications can be met at modes below 4. At higher modes, the measured power spectrum plot is above the new NIF specification plot for capsules with margin, but is below the curve for capsules with no margin. This data indicates that improvements are needed for modes higher than 4.

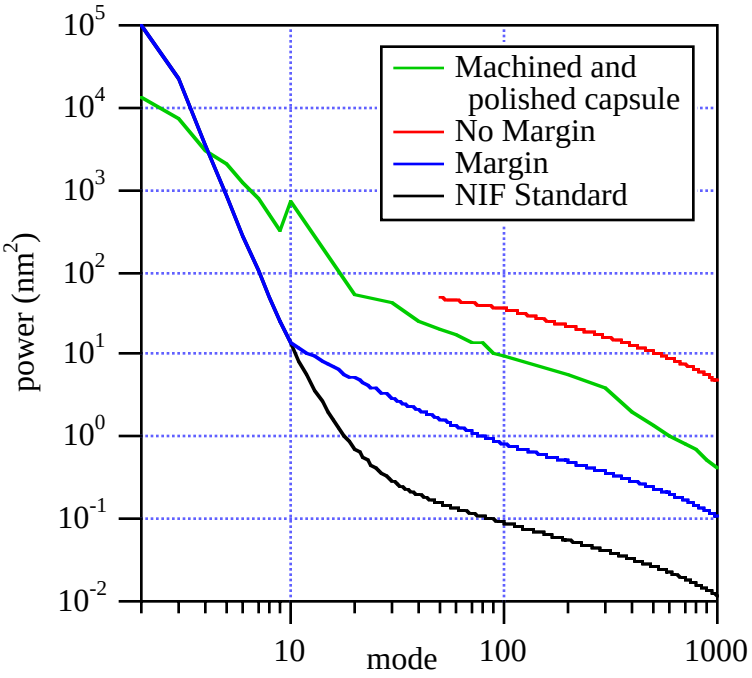


Figure 8. Power spectrum for machined and polished capsule. The NIF Standard curve represents the traditional NIF standard curve. Curves labeled "No Margin" and "Margin" represent new standards for Be0.9%Cu capsule with uniform radial distribution of dopant. The "No Margin" curve represents the power spectrum acceptable if there are no other imperfections in the target, the "Margin" curve allows for expected levels of imperfection in the target.

Improved shape quality at low modes can be achieved with a higher precision lathe. To demonstrate this, aluminum spheres were machined on a new Moore precision lathe. Figure 9 shows the results of these machining tests. The low mode specifications are met below mode 8, and overall the power spectrum is closer to the NIF standard than the previously machined Be0.9%Cu capsule.

The Al sphere machining tests in Figure 9 involved the cutting tool moving in a "two axis" fashion. In this approach the tool is moved along a circular contour by moving both the *x* and *z* axis of the machine in a stepwise fashion to create the desired curved tool path. Since the tool is moved in a stepwise fashion and the point of contact of the sphere to the cutting tool is changing,

this cutting method introduces some error. A preferred method for cutting spheres is to move the tool in a rotary fashion so that the stepwise tool movement is eliminated and the tool contacts the sphere at a single point. Machining spheres in this manner requires a lathe that is equipped with *b*-axis, or rotary cutting capability.

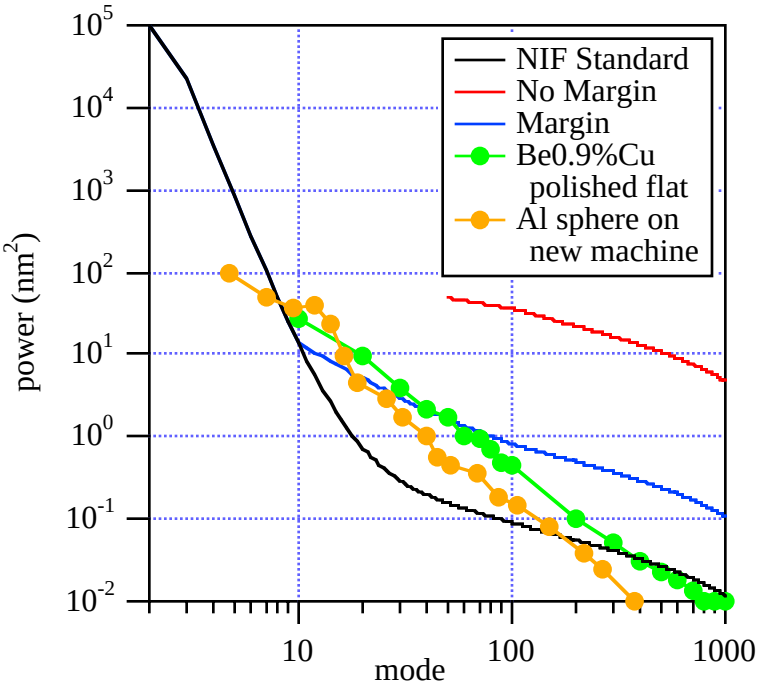


Figure 9. Power spectrum results for a 2 mm Al sphere that was machined by a 2 axis cutting scheme. Also shown is the power spectrum of a polished Be0.9%Cu flat sample that was polished with optimized polishing compound.

LANL has procured a new precision lathe that is equipped with *b*-axis cutting capability. The *b*-axis is a rotary table that holds the tool. With this cutting capability the tool holder can be rotated so that the tool follows a smooth contour rather than the stepwise contour provided by the *x* and *z* axis cutting method. With this method we anticipate that low mode spherical quality will be better than was achieved in the Al sphere cutting tests shown in Figure 9. Work in FY05 will attempt to demonstrate this with the new LANL lathe with both surrogates and Be0.9%Cu.

Solving the high mode problem will involve smoothing high frequency defects such as machine tool features, grain pullout, and material voids. We have performed polishing studies with flat Be and Be0.9%Cu samples to determine the feasibility of smoothing high frequency defects. Polishing of these samples began with relatively rough (160 µm $R_a$) cBN-turned Be and Be0.9%Cu surface finish. Figure 9 shows the results from these studies. The optimum polishing compound was 0.05 µm colloidal silica. Pure Be, which is not shown in Figure 9 can easily be polished to meet the high mode NIF specification in flats, so there are no fundamental materials issues that would prevent achieving smooth surfaces. Polishing results with Be0.9%Cu samples are slightly above the NIF specs, but probably sufficient for ignition capsules. Why Be0.9%Cu cannot be polished as smoothly as Be is not clear, but is likely due to grain pullout or other defects associated with this alloy. About the same result was seen for polishing sputtered Be0.9%Cu. Future improved alloy quality may result in the ability to achieve smoother surfaces.

Machined capsules are cut with cubic boron nitride (cBN) tools. Due to its reactivity with carbon, diamond is known to be incompatible with machining Be. We have, however conducted cutting tests with Be0.9%Cu and found that smooth surfaces (18 nm rms) can be achieved with diamond tools on small (2 mm) samples. Apparently, the small sample size and slow cutting rate does not generate much heat, and the diamond tool does not degrade. This result is encouraging in that it suggests that it may be possible to perform the major cutting operations with cBN, and then perform a final finishing cut with diamond. The polished capsule with power spectrum shown in Figure 8 was obtained by polishing the cBN machined capsule. Further, the polishing was performed with a polishing compound that was not optimized. By starting the polishing operation with a diamond turned surface and by using optimized polishing compound, significantly less polishing should be required to achieve NIF quality surfaces.

Figure 10 shows optical photographs of cBN and diamond machined Be0.9%Cu surfaces. It is clear that diamond machining clearly produces smoother surfaces.

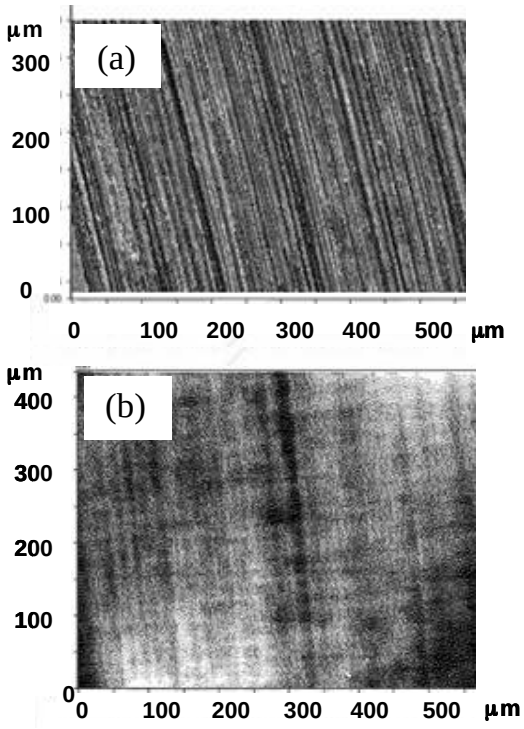


Figure 10. Optical photographs of cBN and diamond machined Be0.9%Cu surfaces produced from ECAE grain refined alloy. (a) Surface machined with cBN tool, surface roughness 152 nm rms. (b) Surface machined with diamond tool, surface roughness 18 nm rms.

From the above, the following can be summarized with respect to achieving NIF capsule shape specifications. Machining tests on a new lathe to produce a 2 mm Al sphere using a stepwise cutting method have demonstrated low mode quality better than the NIF standard for modes less than 8. A newly acquired precision lathe at LANL that has *b* axis cutting capability is expected to provide spheres with better low mode quality than was demonstrated with the Al sphere shown in Figure 9. Experiments with Be0.9%Cu flats have demonstrated that high mode surface finishes acceptable for uniform doped ignition capsules can be achieved by polishing. Polishing to achieve smooth surfaces must now be demonstrated using spheres. This is planned for FY05. Experiments have shown that diamond tools can produce higher quality surface finishes on Be0.9%Cu than cBN tools. These results indicate that it may be possible to use a diamond tool to perform a finishing cut on a capsule, and this would make the spherical polishing job much easier.

The improved low mode quality that will be afforded with the new lathe as well as the use of diamond turning and optimized polishing compounds suggest that large improvements in the spherical power spectrum with respect to that shown in Figure 8 will be realized.

## V. DT filling

Be0.9%Cu capsules fabricated by precision machining would be filled with DT by one of two methods. These filling methods will not be covered in significant detail here. These methods are to fill by use of a fill tube attached to a small laser drilled hole in the capsule. The second fill method would be to cryo-condense DT in the capsule through a small laser drilled hole and the laser seal this hole. These two filling methods are applicable to both sputtered and precision machined Be0.9%Cu capsules.

## VI. Characterization of Be0.9%Cu shells

Characterization of Be0.9%Cu shells will require measuring capsule shape and feature properties, as well as capsule material properties. Shape and feature properties are properties such as capsule surface power spectrum, wall thickness uniformity, interior surface finish, fill hole details and hemishell bond details. Capsule material properties are the fundamental properties of the material, such as x-ray opacity, opacity variation, density, microstructure, chemical composition and thermal properties (thermal conductivity and thermal expansion).

Efforts are underway to establish the capability to make these measurements. Particularly challenging are measurements of x-ray opacity. Opacity must be measured with precision of 1 part in $10^4$ over 50 μm length scale. X-ray absorption methods are being investigated at General Atomics to do this. Measurements of capsule wall thickness must be measured to resolutions of less than one micron. Radiography techniques are being considered for this measurement. Measurements of other fundamental materials properties are straightforward.

## VII. Summary

We are developing the capability to produce Be0.9%Cu capsules based on use of precision machining methods. The ability to cast and grain refine the alloy has been established, and the process for obtaining fine grain material using ECAE is being optimized. 20-50 micron size grains have been achieved in initial demonstrations. Further improvements are expected. Bonding of hemishells is being done and the bonds formed to date are sufficiently strong for room temperature transport of some ignition designs. Improvements in bond strength are expected. Previously machined capsules meet low mode specifications below mode 4. The combination of a new precision lathe, results from diamond turning tests and development of optimum polishing compounds suggests that major improvements to the power spectrum should be seen.

## References

1. R.B. Stephens, S.W. Haan, D.C. Wilson, *Fusion Science and Technology* **41**, 226 (2002).

2. S.W. Haan, T. Dittrich, G. Strobel, S. Hatchett, D. Hinkel, M. Marinak, D. Munro, O. Jones, S. Pollaine, L. Suter, *Fusion Science and Technology* **41**, 164 (2002).

3. D.J. Alexander, J.C. Cooley, D.J. Thoma and A Nobile, "Grain Refinement of Arc-Melted Beryllium-6 wt% Copper", *Ultrafine Grained Materials III*, 267 (2004).

4. D.J. Alexander, J.C. Cooley, D.J. Thoma, A. Nobile, “Production of Fine-Grained Beryllium-6 wt% Copper for Fusion Ignition Capsules by Arc Melting and Equal Channel Angular Extrusion”, *Fusion Science and Technology* **45**, 137 (2004).

5. A. Nobile, J. C. Cooley, D. J. Alexander, D. J. Thoma, R. D. Field, R. D. Day, B. J. Cameron, G. Rivera, A. M. Kelly and P. A. Papin, R.K. Schulze, L. B. Dauelsberg, N. B. Alexander and R. Galix, “Development of Beryllium-Copper Alloy Ignition Capsules”, *Proceedings of the Third International Conference on Inertial Fusion Sciences and Applications*, September 7-12, 2003, p. 758.

6. J. M. Marder, *J. Materials for Energy Systems* **8,** 17 (1986).

## Machined Be Shell Bibliography

L. J. Salzer, V. M. Gomez, J. Moore, J. J. Bartos, P. Gobby, and L. Foreman, "Machining Sub-Millimeter Beryllium and Aluminum Components of Laser Targets," *Fus. Technol*. **28**, 1829 (1995).

D. C. Wilson, P. A. Bradley, N. M. Hoffman, F. J. Swenson, D. P. Smitherman, R. E. Chrien, R. W. Margevicius, D. J. Thoma, L. R. Foreman, J. K. Hoffer, S. R. Goldman, S. E. Caldwell, T. R. Dittrich, S. W. Haan, M. M. Marinak, S. M. Pollaine, and J. J. Sanchez, "The Development and Advantages of Beryllium Capsules for the National Ignition Facility," *Phys. Plasmas.* **5**, 1953 (1998).

R. W. Margevicius, L. J. Salzer, M. A. Salazar, and L. R. Foreman, "Toward the Fabrication of a NIF Target Via Hemisphere Joining," *Fus. Technol*. **35**, 106 (1999).

M. A. Salazar, R. Hermes, and R. W. Margevicius, "Effects of Joining and Testing Parameters on the Adhesive Strength of Epoxy-Bonded Aluminum and Beryllium," *Fus. Technol*. **35,** 119 (1999).

R. Cook, “A Model Study of the Possible Effect of Beryllium Grain Sound Speed Anisotropy on ICF Capsule Implosions,” *Fusion Sci. Technol.* **41**, 155 (2002).

R. W. Margevicius, "Effect of Crystallographic Texture on Sound Velocity Propagation in Polycrystalline Beryllium," *Fusion Sci. Technol.* **41**, 286 (2002).

A. Nobile, J. C. Cooley, D. J. Alexander, D. J. Thoma, R. D. Field, R. D. Day, B. J. Cameron, G. Rivera, A. M. Kelly and P. A. Papin, R.K. Schulze, L. B. Dauelsberg, N. B. Alexander and R. Galix, “Development of Beryllium-Copper Alloy Ignition Capsules”, *Proceedings of the Third International Conference on Inertial Fusion Sciences and Applications*, September 7-12, 2003, p. 758.

A. Nobile, S. C. Dropinski, J. M. Edwards, G. Rivera, R. W. Margevicius, R. J. Sebring, R. E. Olson, and D. L. Tanner, "Fabrication and Characterization of Targets for Shock Propagation and Radiation Burnthrough Measurements on Be-0.9AT.%Cu Alloy," *Fus. Sci. Technol.* **45**, 127 (2004).

D.J. Alexander, J.C. Cooley, D.J. Thoma and A Nobile, “Grain Refinement of Arc-Melted Beryllium-6 wt% Copper”, *Ultrafine Grained Materials III*, 267 (2004).

D.J. Alexander, J.C. Cooley, D.J. Thoma, A. Nobile, “Production of Fine-Grained Beryllium-6 wt% Copper for Fusion Ignition Capsules by Arc Melting and Equal Channel Angular Extrusion”, *Fusion Science and Technology* **45**, 137 (2004).

## Ge-doped CH/CD Capsules

In this preliminary evaluation of fabrication of Ge-doped CH shells for the National Ignition Facility (NIF), we report the method of fabrication and the current status and unresolved issues. In particular, we discuss the evaluation of the surface finish of full thickness CH shells. Infrared (IR) absorption properties, important for cryogenic layering of this ablator material, are also discussed.

### Fabrication technique

The Ge-doped CH/CD ablator material is produced by chemical vapor deposition of a polymer in vacuum plasma. This process is commonly referred to as plasma polymerization and was first developed for ICF target fabrication over twenty years ago.[1] In this process, a hydrocarbon gas, the precursor, is broken down in an inductively coupled plasma system. The fragments deposit on the substrates and form a pure CH polymer film as shown in Figure 1. The addition of excess hydrogen gas to the process is essential in obtaining smooth, virtually stress-free films at the thicknesses required for ICF laser implosions (tens to over a hundred μm). Deuterated films (CD) are obtained by changing the precursor hydrocarbon gas to its fully deuterated analog (as well as using $D_2$ instead of hydrogen). Dopants are incorporated by adding a precursor gas or vapor containing the desired dopant atom. For example, for germanium, the vapor of tetramethyl germanium (TMG) is added to the basic process used for undoped coatings.[2] The relative concentration of TMG in the process controls the level of doping. The coating rate is about 0.3-0.5 μm/hr, requiring over two weeks to deposit the full NIF thickness of ~ 150 μm.

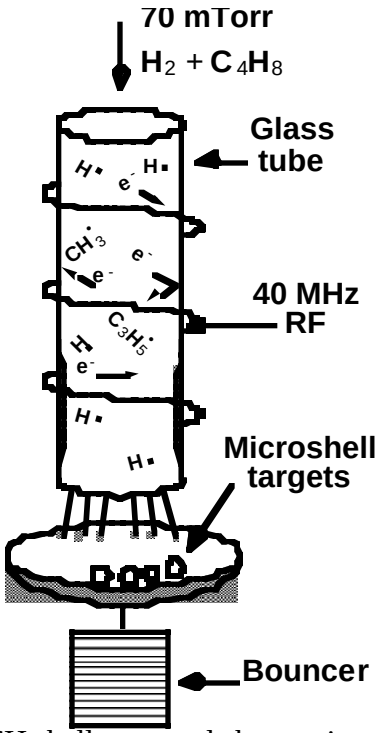


Figure 1. Full thickness CH shells are made by coating appropriate mandrels with CH polymer using the plasma polymerization technique shown in the figure. Hydrocarbon precursors are broken down in the plasma and deposit on the substrates and form a polymer. Hydrogen is used to obtain smoother surfaces. The coatings can be doped by adding the vapor of a hydrocarbon containing dopant.

Ge-doped CH is deposited on spherical mandrels. The mandrel is typically poly-alpha-methylstyrene (PAMS) which is produced by microencapsulation.[3] This mandrel may be thermally removed early in the coating operation. Uniform coating of mandrels requires agitation during deposition of the Ge-doped CH coating. Typically mandrels are placed in a pan attached to a piezo electric shaker to provide this required agitation during coating. However, for NIF size shells (~ 2 mm diameter) another agitation scheme is used where the coating pan is tapped every few minutes during the coating.[4] This avoids the agitation-induced defects observed when the piezo shaking technique is used. Typically 10 mandrels can be coated in a single coating run.

The fabricated shells are characterized by a variety of techniques including microscopy, white light interferometry and the Atomic Force Microscope (AFM) spheremapper. The AFM spheremapper provides the most important metrology data used to evaluate the quality of the shell. The AFM -produced power spectra of the shells are compared to the desired spectrum, "the NIF standard", provided by current designs. The AFM spheremaps are generally performed by mapping the shell in 3 closely spaced traces about 3 orthogonal axes. This operation can be performed in about 30 minutes. The "full spheremap" technique (70 traces in each of 5 axes) allows much more detailed examination of the surface, especially in high modes, but the operation is much more time consuming, typically requiring 5 hours per shell. We mainly used the standard AFM spheremapping and reserved the "full spheremap" for the best shells.

**Surface finish**

Our evaluation has focused on pure CH coatings. Previous data on Ge-doped CH coatings indicate that the surface finish for the two materials evolves very similarly, with the Ge dopant having little or no effect. We have found no major issues in producing the full thickness shells, such as coater, agitation or other system failures during the long coatings. We are able to produce shells with surface power spectra near or below the "NIF standard" as shown in Figure 2. However typically fewer than 10% of shells in any batch were near the "NIF standard." The major defects on full thickness CH shells that result in excess power in the modal spectra are isolated dome-like features.

There are several possible sources for the surface finish of the full thickness shells not meeting the NIF standard. One is the plasma polymer coating process itself. The second is the quality of the mandrel. Any low mode features on the mandrel will be reproduced on the final shell. Also, any high mode roughness or isolated defects present on the mandrels grow during the coating and degrade the surface finish of the full thickness shell. The third is any isolated defects produced during the coating due to agitation. Finally, there is the cleanliness of the process in each of its steps. We examined each of these possibilities as part of our evaluation as discussed in the following.

The coating process itself had been previously examined numerous times on thick coatings on flat substrates,[5] as well as coatings on smaller shells (~ 1mm diameter).[6] These examinations had indicated that it is suitable for ICF target fabrication, yielding RMS surface finish of a few nm for coatings over 100 μm thick, consistent with the "NIF standard" requirement. The surface finish here refers to the ubiquitous background finish, ignoring any isolated features on the surface. It is usually measured by coating on ultra-smooth surfaces such as freshly cleaved mica. Coating on such ultra-smooth surfaces also indicates that the coating process itself does not generate any isolated defects such as dome-like structures. However, fine tuning of the coating parameters is required for a given plasma polymer coater to obtain the desired surface finish. Such optimization was carried out on the coater designated for this work to obtain thick coatings with the desired few nm RMS background surface finish without presence of any isolated domes. Indeed the background surface finish on full thickness shells produced throughout our evaluation was as desired.

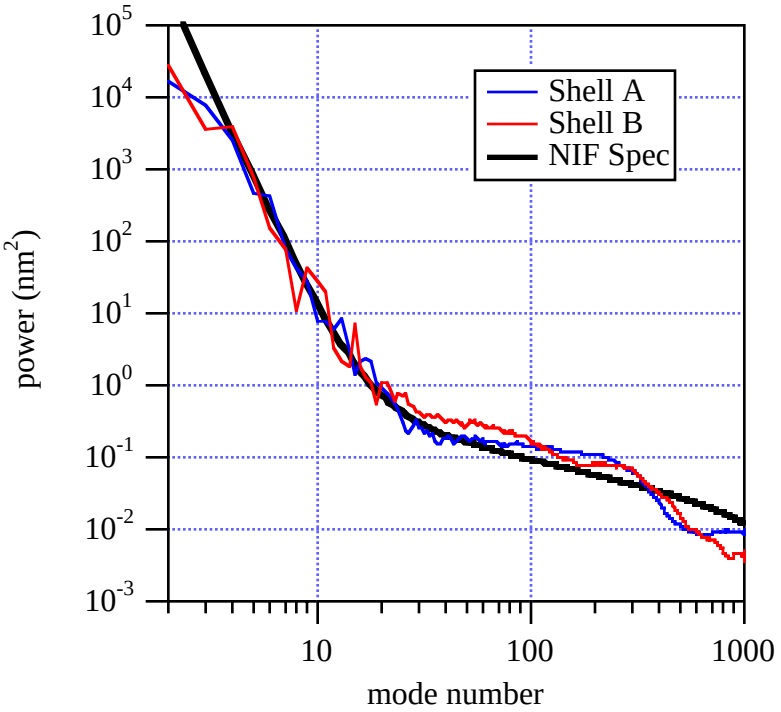


Figure 2. Full thickness CH shells very nearly meeting the "NIF standard" were produced in FY04 using plasma polymerization coating technique. The yield of such shells, however, has been low (~10%) due to the presence of large isolated features on the shells.

The other causes of surface degradation are isolated features in the form of domes and are the main issue remaining with fabrication of "NIF quality" full thickness CH shells *routinely*. The AFM surface profile shown in Figure 3 illustrates this problem. The majority of these domes are typically a few μm wide and a few tenths of μm tall. These smaller domes do not degrade the power spectrum significantly. However, larger domes, mainly those ~ one μm in height or taller, while much lower in density, do lead to significant increase in the power spectrum well beyond the NIF standard. Two of the possible causes of dome generation, large or small, are 1) seeds on the mandrels introduced in the their fabrication and 2) possible agitation induced defects during coating. The quality of the mandrels used for coatings is batch dependent. Also, agitation during coating has been shown to induce such defects.[4] We attempted to separate these two causes, and have shown that the agitation during the coating process is not the major cause of dome generation.

We examined coatings on mandrel batches using shorter (~ 6-7 day, ~ 70 μm thickness) coating runs. Only mandrels from those batches with shells consistently meeting the "NIF standard" were used. To distinguish between mandrel defects and agitation induced defects, mandrels from several different batches were coated in the *same* coating run. Shells from some batches produced poorer surfaces than others indicating a problem with those particular batches. Through this culling process we identified superior batches and only they were used in any further work. To further separate the cause of dome generation, coated shells from the remaining batches were coated for another week, reaching full thickness. Only a slight increase in the number of domes was observed in doubling the thickness, indicating the coating process was not the main source of dome generation. Coatings of fixed mandrels, i.e. those coated *without* any agitation, also showed growth of domes from the mandrel surface. It was concluded that the majority of isolated features were produced from seeds present on the mandrel. However, most of these domes were in the few tenths of μm and we could not explain the presence of taller domes.

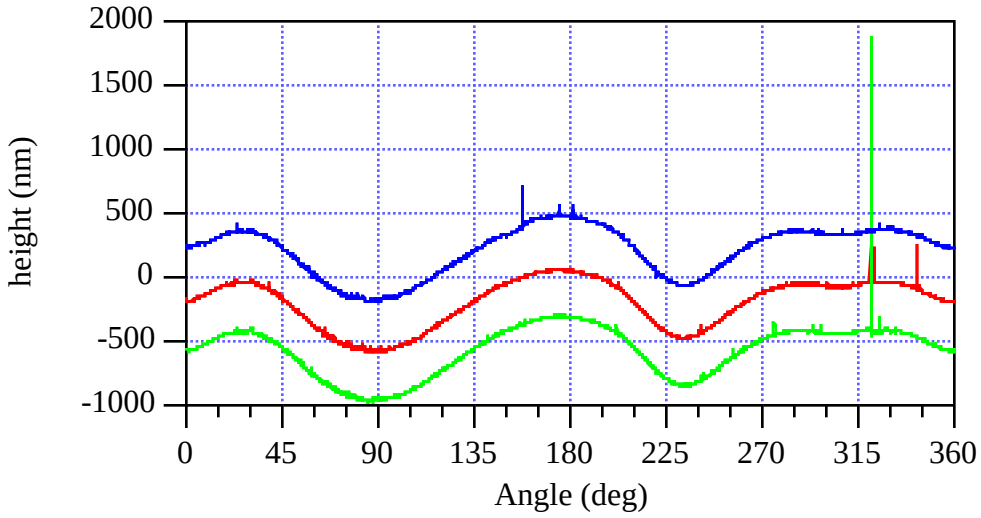


Figure 3. This figure shows the surface height deviation as a function of angle as mapped by the AFM spheremapper. The major cause of excess power in the modal spectrum of full thickness CH shells are the large spikes (for example at ~ 320 deg) in the AFM trace. This spike is due to an isolated dome. Note also the smaller spikes corresponding to domes only a few tenths of μm tall. These features do not significantly affect the power spectrum.

We are investigating the possibility that lack of clean handling of shells prior to and post coating is the major source of such taller domes. Post coating debris is distinguished as being free to move on the surface and it can be detected optically as loose debris. Also shells are handled much more cleanly after the coating prior to AFM examination. Most of the tall domes we have observed are firmly attached to the shell surface and therefore the seeds were present prior to coating. The lack of thorough clean handling in our process has been dictated by the necessity of examining mandrels carefully prior to coating to eliminate "mid-mode" defects. Eliminating this screening examination has resulted in reduced high mode roughness on the majority of shells coated as seen in Figure 4. The presence of the somewhat large middle mode power in the red spectrum shown is the direct result of not examining the mandrels prior to coating. We have performed a "full spheremap" of these shells and compared them to the best obtained with standard handling. This is shown in Figure 5. The number of large spikes seen in the expanded surface scale is significantly fewer in the case of clean handling. We are in the process of moving the mandrel screening into a clean environment.

**IR Absorption**

The full NIF target will have a solid ice layer of DT fuel inside the ablator material. The quality of the DT ice layer can be enhanced beyond the natural β-layering process by heating the ice with infrared light (IR) tuned to a $D_2$ or DT excitation band. The IR must pass through the capsule wall, and absorption heats the capsule material, which is deleterious both in terms of reducing the energy input to the ice as well as increasing the difficulty of symmetrically cooling the capsule. To optimize the choice of wavelength we measured the wavelength dependent transmission properties of IR through both CH and CD.[7] The results are shown in Figure 4 in the polyimide section. The absorption at the DT absorption maximum (wavelength ~ 2900 $cm^{-1}$) is lowest for CD coatings. The best current value for the CD absorption coefficient is about 20 $cm^{-1}$. This residual absorption is presumably due to CH impurities in the deuterated precursors used for CD coatings. Prospects for lowering these values for deuterated materials based on increasing the

isotopic purity may lead to a 25-50% reduction. With best current values of about 20 $cm^{-1}$ it is estimated that we can add 2-4 times the nominal β-layering energy to the DT ice. Reductions in the extinction coefficient from increases in isotopic purity and improved processing conditions might increase the ice heating, allowing us to maintain the ice surface smoothness as we lower the temperature to reduce the gas density.

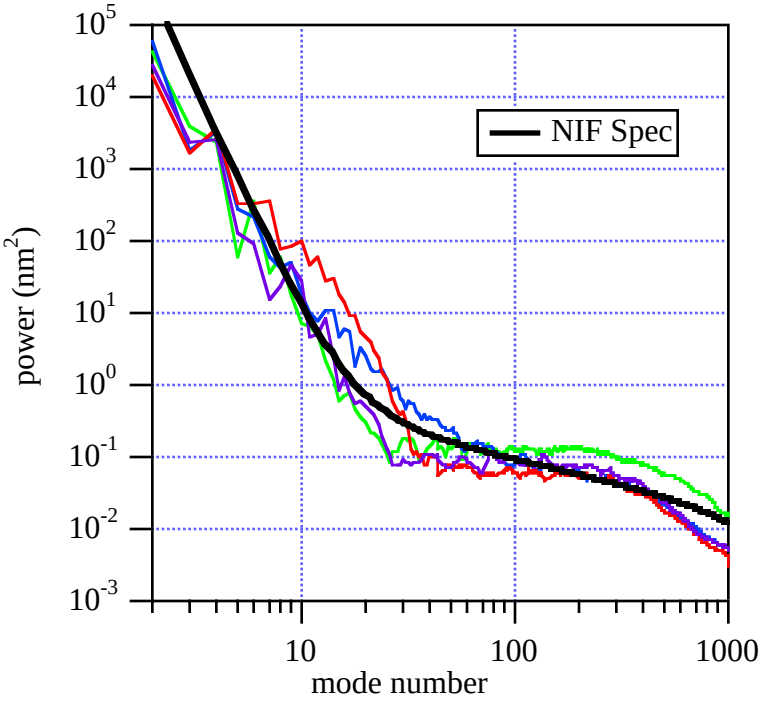


Figure 4. Example of AFM power spectra of full thickness CH shells made using complete clean handling. The high modes for over 50% of shells were at or near the NIF curve. The middle mode power in the red shell is result of not pre-selecting the mandrels for coating (to avoid particulate pick up during selection in a non-clean environment).

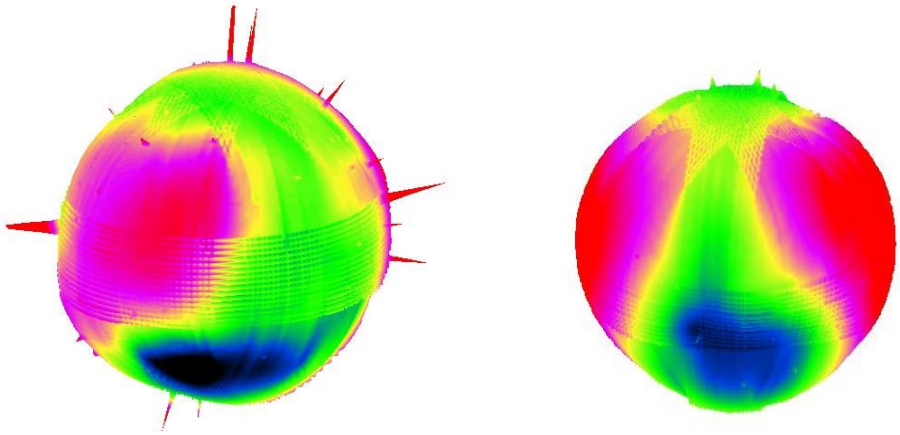

Figure 5. On the left is a "full spheremap" of one of the shells having a 3 axis spheremap spectrum meeting the NIF standard produced not using complete clean handling produced earlier in FY04. Note the large spikes detected with more through examination in the "full spheremap." On the right is a similar image of one of the shells having a 3 axis spheremap spectrum meeting the NIF standard produced recently using complete clean handling. The number of large spikes has been substantially reduced. In both cases the scale is expanded by 300x in the radial direction.

**References**

1. S. A. Letts, D. W. Myers, and L. A. Witt, "Ultrasmooth Plasma Polymerized Coatings for Laser Fusion Targets," *J. Vac. Sci. Technol*. **19**, 739 (1981).

2. R. Brusasco, M. Saculla, and R. Cook, "Preparation of Germanium Doped Plasma Polymerized Coatings as Inertial Confinement Fusion Target Ablators," *J. Vac Sci. Technol. A* **13**, 948 (1995).

3. M. Takagi, R. Cook, B. McQuillan, F. Elsner, R. Stephens, A. Nikroo, J. Gibson, and S. Paguio, "Development of High Quality Poly(α-Methylstyrene) Mandrels for NIF," *Fus. Sci. Technol*. **41**, 278 (2002).

4. A. Nikroo and D. Woodhouse, **"**Bounce Coating Induced Domes on Glow Discharge Polymer Coated Shells," *Fus. Technol.* **35**, 202 (1999).

5. G. W. Collins, S. A. Letts, E. M. Fearon, R. L. McEachern, and T. P. Bernat, "Surface Roughness Scaling of Plasma Polymer Films," *Phys. Rev. Lett.* **73**, 708 (1994).

6. A. Nikroo, J. Pontelandolfo, and E. Castillo, "Coating and Mandrel Effects on Fabrication of Glow Discharge Polymer NIF Scale Indirect Drive Capsules," *Fus. Sci. Technol*. **41**, 220 (2002).

7. R. Cook, M. Anthamatten, S. A. Letts, A. Nikroo, and D. G. Czechowicz. "IR Absorptive Properties of Plastic Materials Used in ICF Capsules," *Fusion Sci. Technol.* **45**, 148 (2004).

## GDP Shell Bibliography

S. A. Letts, D. W. Myers, and L. A. Witt, "Ultrasmooth Plasma Polymerized Coatings for Laser Fusion Targets," *J. Vac. Sci. Technol*. **19**, 739 (1981).

G. Devine, S. Letts, R. Brusasco, and R. Cook, "A State-of-the-Art Plasma Polymerization Coater for ICF Targets," *Polymer Preprints* **34,** 671 (1993).

S. A. Letts, P. Welch, R. McEachern, E. Fearon, and R. Cook, "Effect of Process Parameters on Plasma Polymer Surface Finish," *Polymer Preprints* **34,** 671 (1993).

R. Cook, T. P. Bernat, G. Collins, S. A. Letts, R. McEachern, G. E. Overturf, and R. E. Turner, "Production and Characterization of ICF Capsules," in *Proceedings of the 14th International Conference on Plasma Physics and Controlled Nuclear Fusion Research held by the IAEA*, vol. 3, pp 449-54, (1993).

R. Cook, R. McEachern, C. Moore, G. E. Overturf, and S. R. Buckley. "Precision Targets for Precision Nova," *ICF Quarterly Report* **4**, 25 (1993).

G. W. Collins, S. A. Letts, E. M. Fearon, R. L. McEachern, and T. P. Bernat, "Surface Roughness Scaling of Plasma Polymer Films," *Phys. Rev. Lett.* **73**, 708 (1994).

R. Brusasco, M. Saculla, and R. Cook, "Preparation of Germanium Doped Plasma Polymerized Coatings as Inertial Confinement Fusion Target Ablators," *J. Vac Sci. Technol. A* **13**, 948 (1995).

S. A. Letts, E. M. Fearon, S. R. Buckley, M. D. Saculla, L. M. Allison, and R. Cook, "Preparation of Hollow Shell ICF Targets Using a Depolymerizable Mandrel," in *Mat. Res. Soc. Symp. Proc.* **372**, 125 (1995).

R. Cook “Creating Microsphere Targets for Inertial Confinement Fusion Experiments,” *Energy & Technology Review*, (Lawrence Livermore National Laboratory, Livermore, CA), April, 1995, pp 1-9.

S. A. Letts, E. M. Fearon, S. R. Buckley, M. D. Saculla, L. M. Allison, and R. Cook, “Fabrication of Hollow Shell ICF Targets using a Depolymerizable Mandrel,” *Fusion Technol.* **28**, 1797 (1995).

S. A. Letts, E. M. Fearon, L. M. Allison, and R. Cook, “Fabrication of Special Inertial Confinement Fusion Targets Using a Depolymerizable Mandrel Technique,” *J. Vac. Sci. Technol. A* **14**, 1015 (1996).

R. Brusasco, S. Letts, P. Miller, M. Saculla, and R. Cook, “Preparation and Characterization of Beryllium Doped Organic Plasma Polymer Coatings,” *J. Vac. Sci. Technol. A* **14**, 1019 (1996).

Evelyn M. Fearon, Stephan A. Letts, Leslie M. Allison, and R. Cook, “Adapting the Decomposable Mandrel Technique to Build Specialty ICF Targets,” *Fusion Technol.* **31**, 406 (1997).

A. Nikroo, "Deposition and Characteristics of Chlorine-Doped Glow Discharge Polymer Films," *Fusion Technol.* **31**, 431 (1997).

A. Nikroo and D. Woodhouse, **“**Bounce Coating Induced Domes on Glow Discharge Polymer Coated Shells,” *Fus. Technol.* **35**, 202 (1999).

A. Nikroo and J. M. Pontelandolfo, "Fabrication of Thin Walled Glow Discharge Polymer Shells," *Fusion Technol.* **38**, 58 (2000).

M. Theobold, P. Baclet, O. Legaie, and J. Durand, "Properties of a-C:H Coatings Prepared by PECVD for Laser Fusion Targets," *Fusion Technol.* **38**, 62 (2000).

D. G. Czechowicz, E. R. Castillo, and A. Nikroo, "Compositional and Structural Studies of Strong Glow Discharge Polymer," *Fusion Sci. Technol.* **41**, 188 (2002).

A. Nikroo, D. G. Czechowicz, E. R. Castillo, and J. M. Pontelandolfo, "Recent Progress in Fabrication of High-Strength Glow Discharge Polymer Shells by Optimization of Coating Parameters," *Fusion Sci. Technol.* **41**, 214 (2002).

A. Nikroo, J. M. Pontelandolfo, and E. R. Castillo, "Coating and Mandrel Effects on Fabrication of Glow Discharge Polymer NIF Scale Indirect Drive Capsules," *Fusion Sci. Technol.* **41**, 220 (2002).

M. Theobold, O. Legaie, P. Baclet, and A. Nikroo, "Thick GDP Microshells for LIL and LMJ Targets," *Fusion Sci. Technol.* **41**, 238 (2002).

B. Dumay, E. Finot, M. Theobold, O. Legaie, J. Durand, P. Baclet, and J. P. Goudonnet, "Structure of Amorphous Hydrogenated Carbon Films Prepared by Radio Frequency Plasma Enhanced Chemical Vapor Deposition. An Analogy with the Structure Zone Model Developed for Metals," *J. Appl. Phys.* **92**, 6572 (2002).

R. Cook, M. Anthamatten, J. P. Armstrong, S. A. Letts, R. L. McEachern, B. W. McQuillan, and M. Takagi. “Recent Progress in the Development of Capsule Targets for the National Ignition Facility,” *Proc. of the SPIE* **5228**, 692 (2003).

R. Cook, M. Anthamatten, S. A. Letts, A. Nikroo, and D. G. Czechowicz. “IR Absorptive Properties of Plastic Materials Used in ICF Capsules,” *Fusion Sci. Technol.* **45**, 148 (2004).

M. Theobold, B. Dumay, C. Chicanmne, J. Barnouin, O. Legaie, and P. Baclet, "Roughness Optimization at High Modes for GDP CHx Microshells," *Fusion Sci. Technol.* **45**, 176 (2004).

## Polyimide Capsules

### Introduction

We have developed an evaporative deposition technique for thick polyimide (PI) ablator layers for ICF targets. The technique uses stoichiometrically controlled fluxes from two Knudsen cell evaporators containing a dianhydride and a diamine to deposit a polyamic acid (PAA) coating (Figure 1). Heating the PAA coating to 300°C converts it to a polyimide as in Figure 2. Coated shells are rough due to particles on the substrate mandrels and from damage to the coating caused by the agitation used to achieve a uniform coating. We have developed a smoothing process that exposes a rough PAA coated shell to solvent vapor using gas levitation (Figure 3). We found that after smoothing the coatings developed a number of wide (low-mode) defects. We have identified two major contributors to low-mode roughness: surface hydrolysis, and deformation during drying/curing. By minimizing air exposure prior to vapor smoothing, avoiding excess solvent sorption during vapor smoothing, and using slow drying we are able to deposit and vapor smooth coatings 160 µm thick with a surface roughness less than 20 nm RMS.

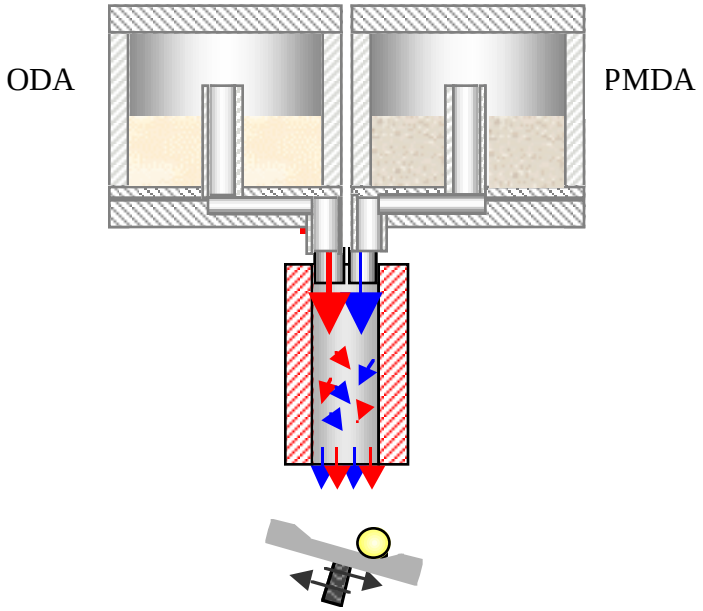


Figure 1. Monomers are loaded into the evaporators above exit through tubes at the base into a mix nozzle. The capsule is agitated in a pan below the mix nozzle.

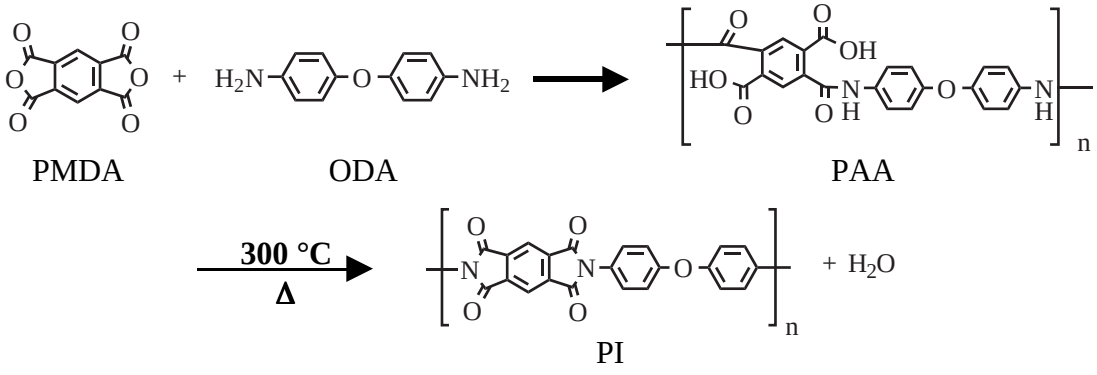


Figure 2. Basic chemistry for the polyimide ablator deposition.

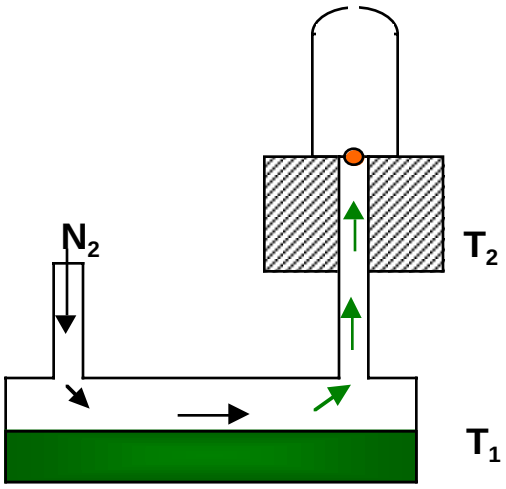


Figure 3. Nitrogen gas passes over a heated solvent bath before levitating the PAA coated shell in a second heated zone.

A polyimide (PI) coating offers a number of advantages as an ablator for inertial confinement fusion (ICF) targets. Polyimide is able to tolerate the radiation exposure from the DT fuel during target fill. PI has a relatively high density that should help reduce Raleigh-Taylor (RT) instabilities, but experiments on planar samples have not agreed with simulations. PI is sufficiently transparent to allow optical characterization of frozen hydrogen fuel layers. The permeability to hydrogen is moderate allowing both fill in a reasonable time and holding capability at low temperature after fill. One problem with PI is that gradient doping to improve RT stability is not possible because of the already large oxygen content.

**Evaporative Coating**

Vapor deposition of PI produces a highly uniform coating thickness when the shell is tumbled randomly in the coating flux. We thus coat spherical shell mandrels made by the depolymerizing mandrel technique with poly(amic acid) (PAA) and then thermally imidize the deposited layer. The evaporative coating system consists of a vacuum system equipped with a diffusion pump and liquid nitrogen trap capable of achieving $10^{-7}$ Torr. Two evaporators and a shell shaking system are contained within a cylindrical chamber. The monomers used are pyromellitic dianhydride (PMDA) and 4,4'oxydianiline (ODA). The dianhydride and the diamine react on the surface to form a polyamic acid (PAA). The polyamic acid is thermally converted to polyimide (PI) with loss of 2 molecules of water per repeat. The evaporators delivering PMDA and ODA are heated to 192 and 172°C respectively. Monomer delivery rate is 0.25 g/h, which results in a coating rate on a rolling spherical substrate of 8 µm/h. These temperatures result in a PMDA/ODA molar ratio (based on material delivered from the evaporator cells) of about 1.3. This ratio is not what is coated on the shell due to preferential reemission of the PMDA. We find that coatings with lower molar ratios tend to develop ODA crystals on the outer surface after cure.

**Deuterated PI**

One method for improving the uniformity of the frozen DT fuel inside cryogenic implosion capsules is to radiantly heat the DT with infrared energy. It is important to dissipate the energy primarily in the fuel and not in the capsule wall. This requires that the capsule ablator material should not absorb the incident radiant energy. One way to make the ablator highly transmissive in the spectral region in which DT absorbs energy is to prepare deuterated polymer. The necessary deuterated monomers for our vapor deposition process were custom synthesized. The same evaporation conditions were used as for the hydrogen analogs. Films from 5 to 100 µm thick were

measured for IR transmission. The results for regular and deuterated PI (PIH and PID), along with those of regular and deuterated plasma polymer (CH and CD), are shown in Figure 4.

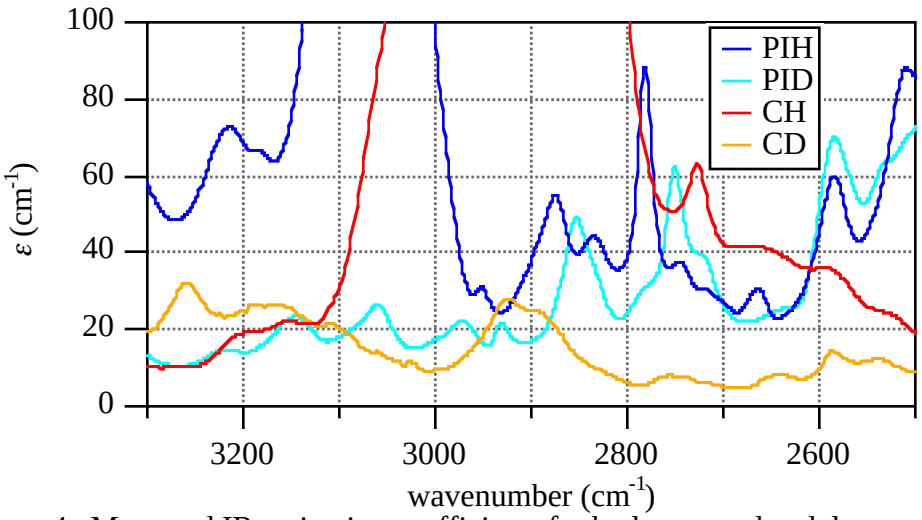


Figure 4. Measured IR extinction coefficients for hydrogenated and deuterated polyimide (PIH and PID) and plasma polymer (CH and CD).

**Solvent-Vapor Smoothing**

We have found that the vapor deposited coatings have roughness from various sources, including particles on the substrate and abrasion of the fragile PAA coating caused by agitation in the shaking pan. To remove the roughness in the as-deposited shells, we have developed a solvent-vapor smoothing process shown in Figure 3. The smoothing technique exposes a gas-levitated capsule to solvent vapor, which causes the polymer to swell. The swollen PAA has a reduced viscosity, which allows surface roughness to flow driven by surface tension. The smoothing technique is most effective in removing high-frequency defects. We have found that our effort to smooth occasionally produced unacceptable low frequency roughness. We now have an understanding of two major roughness-generating mechanisms caused by hydrolysis and buckling and have been able to eliminate these defect sources.

Poly(amic acid) is susceptible to hydrolysis. Our initial handling of coated samples included venting the vacuum system to nitrogen followed by characterization of the coating in air that could take up to several hours. A common feature observed in air-exposed shells is the pit structure observed in AFM traces. The typical characteristics of the pit feature is a depression from 1 to 2 µm in depth surrounded by a mound of material resembling a crater with a diameter of about 500 µm (mode 15). We believe this type of feature is the result of de-wetting. Hydrolysis may produce a surface layer with a higher surface energy than the unhydrolyzed material beneath. During solvent vapor smoothing the higher surface energy, low viscosity hydrolyzed outer layer can deform, and may minimize its surface free energy by de-wetting from the lower surface energy material below. This potentially causes several forms of roughening including pit formation as well as a general wrinkling of the surface. We have now modified our handling and characterization procedures to limit the time that the as-coated shells spend exposed to ambient air conditions before smoothing and curing. By limiting air exposure we have completely eliminated pit defects and greatly improved smoothing yield.

A series of experiments were conducted with the vapor smoothing apparatus to investigate the effects of reservoir temperature, shell temperature and exposure time. It was found that conditions that caused large solvent absorption by the shell, followed by rapid drying, led to the

formation of shell deformation with a "golf ball" appearance. In some cases the buckling is very subtle and only shows up when the shell is carefully examined by microscopy. Radiographs of these golf ball shells show that the low mode roughness is on the inside surface. A possible mechanism for forming this structure is related to the drying rate. When a shell is dried rapidly the outer surface looses nearly all solvent and begins to cure and contract. The contraction produces a pressure on the inner mandrel layer that is transmitted through a solvated fluid layer that has not yet dried. The pressure may then cause the inner mandrel to buckle. To eliminate this buckling we have reduced the solvent uptake of the PAA layer and are using a slower drying rate.

## Reproducibility

We have improved reproducibility by improving both the coater and the smoother operation.. The coater stability, uniformity and shell motion were improved through better thermal control, use of a vapor mixing device and constrained motion of the shell in a pan. The smoother problems were related to smoother vapor exposure conditions and defects discovered after performing smoothing. By conducting experiments that quantified the depth of penetration of solvent as a function of operating conditions we were able to adjust the smoothing apparatus to give consistent performance. Other smoothing failures were related to surface hydrolysis, which caused surface de-wetting. Rapid drying caused buckling of the inner mandrel, which was eliminated by choosing a slower thermal ramp. Crystals on the surface were found to occur in ODA rich coatings. Coating using an excess of PMDA solved this problem. After discovering the causes and solutions for several coating and smoothing distortion mechanisms our ability to recognize, interpret and prevent most defects allowed us to avoid these failures and greatly improve process yield.

Using our improved process knowledge we were able to steadily produce excellent quality vapor smoothed PI shells. The most demanding measure of the sphericity and smoothness of the PI coating is to perform an AFM sphere map. The coated shell is mounted on a precision air-bearing spindle and rotated while the surface contour is sensed using an AFM probe. Three circumferential scans separated by 10 μm are taken in three orthogonal scan directions. The traces are Fourier transformed and graphed as a spectrum of power (square of the Fourier amplitude) as a function of mode number (frequency). Figure 5 shows the average power spectra for several recent solvent vapor smoothed PI coatings. The smoothed limited air exposure shells are among the best we have ever produced with 140-180 μm polyimide thicknesses.

## Conclusion

Polyimide coated shells have continued to improve through process enhancements and the discovery and control of deformation mechanisms. We have found that coating composition uniformity was improved by tilting the pan to spatially constrain the shell location, and by using a mix chamber to eliminate concentration gradients from the evaporators. Hydrolysis of the coated PAA by exposure to air prior to vapor smoothing was found to degrade and roughen the surface, possibly by a de-wetting mechanism. Buckling of the inner mandrel can occur during smoothing by a combination of having high solvent sorption and rapid drying. Contraction of the outer layer applies a pressure at the inner mandrel and causes it to deform by buckling. Using the mix chamber on the evaporators, minimum air exposure conditions prior to vapor smoothing, and slow drying after smoothing we are able to produce shells with a power spectrum matching the mandrel and meeting the NIF standard.

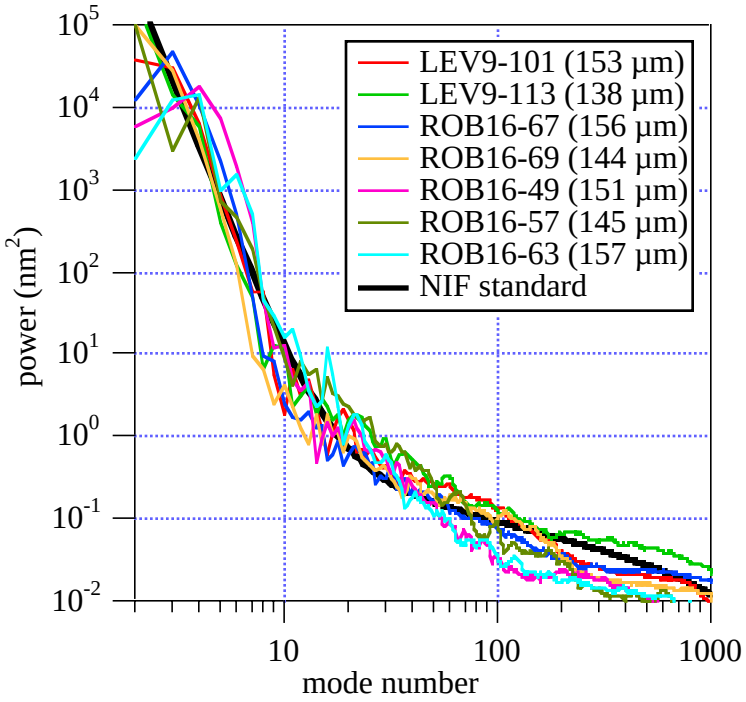


Figure 5. Power spectra of some recent full thickness polyimide shells. The black line represents the design goal.

## Polyimide Shell Bibliography

J. J. Sanchez and S. A. Letts, "Polyimide Capsules May Hold DT Fuel Without Cryogenic Support for the National Ignition Facility Indirect-Drive Targets," *Fusion Technol.* **31**, 491 (1997).

E. L. Alfonso, S. H. Chen, R. Q. Gram, and D. R. Harding, "Properties of Polyimide Shells Made Using Vapor Phase Deposition," *J. of Mater. Res.* **13**, 2988 (1998).

E. L. Alfonso, F.-Y. Tsai, S. H. Chen, R. Q. Gram, and D. R. Harding, "Fabrication of Polyimide Shells by Vapor Phase Deposition for Use as ICF Targets," *Fusion Technol.* **35,** 131 (1999).

C. C. Roberts, S. A. Letts, M. D. Saculla, E. J. Hsieh, and R. Cook, "Polyimide Films from Vapor Deposition: Toward High Strength NIF Capsules," *Fusion Technol.* **35**, 138 (1999).

R. Cook, "Models of Polyimide Spray Coatings," *Fusion Technol.* **38**, 74 (2000).

F.-Y. Tsai, E. L. Alfonso, S. H. Chen, and D. R. Harding, "Mechanical Properties and Gas Permeability of Polyimide Shells Fabricated by the Vapor Deposition Method," *Fusion Technol.* **38,** 83 (2000).

C. C. Roberts, P. J. Orthion, A. E. Hassel, B. K. Parrish, S. R. Buckley, E. Fearon, S. A. Letts, and R. Cook, "Development of Polyimide Ablators for NIF: Analysis of Defects on Shells, a Novel Smoothing Technique and Upilex Coatings," *Fusion Technol.* **38**, 94 (2000).

F.-Y. Tsai, E. L. Alfonso, D. R. Harding, and S. H. Chen, "Processing Vapour-Deposited Polyimide," *J. Phys. D-Appl. Phys.* **34**, 3011 (2001).

F.-Y. Tsai, D. R. Harding, S. H. Chen, T. N. Blanton, and E. L. Alfonso, “Effects of Processing Conditions on the Quality and Properties of Vapor-Deposited Polyimide Shells,” *Fusion Technol.* **41**, 178 (2002).

S. A. Letts, A. E. H. Nissen, P. J. Orthion, S. R. Buckley, E. Fearon, C. Chancellor, C. C. Roberts, B. K. Parrish, and R. Cook, “Vapor-Deposited Polyimide Ablators for NIF: Effects of Deposition Process Parameters and Solvent Vapor Smoothing on Capsule Surface Finish,” *Fusion Sci. Technol.* **41**, 268 (2002).

A. P. Gies, W. K. Nonidez, M. Anthamatten, R. Cook, and J. W. Mays “Characterization of an Insoluble Polyimide Oligomer by Matrix-Assisted Laser Desorption/Ionization Time-of-Flight Mass Spectrometry,” *Rapid Commun. Mass Spectrom.* **16**, 1903 (2002).

F.-Y. Tsai, T. N. Blanton, D. R. Harding, and S. H. Chen, “Temperature Dependence of the Properties of Vapor-Deposited Polyimide,” *J. of Appl, Phys.* **93**, 3760 (2003).

F.-Y. Tsai, D. R. Harding, S. H. Chen, and T. N. Blanton, “High-Permeability Fluorinated Polyimide Microcapsules by Vapor Deposition Polymerization,” *Polymer* **44**, 995 (2003).

R. Cook, M. Anthamatten, S. A. Letts, A. Nikroo, and D. G. Czechowicz. “IR Absorptive Properties of Plastic Materials Used in ICF Capsules,” *Fusion Sci. Technol.* **45**, 148 (2004).

S. A. Letts, M. Anthamatten, S. R. Buckley, E. Fearon, A. E. H. Nissen, and R. Cook, “Progress Toward Meeting NIF Specifications for Vapor Deposited Polyimide Ablator Coatings,” *Fusion Sci. Technol.* **45**, 180 (2004).

A. K. Knight, F.-Y. Tsai, M. J. Bonino, D. R. Harding, "Suitability of Different Polyimide Capsule Material for Use as ICF Targets, *Fusion Sci. Technol.* **45**, 187 (2004).

M. Anthamatten, S. A. Letts, and R. Cook, “Controlling Surface Roughness in Vapor-Deposited Poly(amic acid) Films by Solvent-Vapor Exposure,” *Langmuir* **20**, 6288 (2004).

A. P. Gies, W. K. Nonidez, M. Anthamatten, and R. Cook, “A Matrix-Assisted Laser Desorption/Ionization Time-of-Flight Mass Spectrometry Study of the Imidization of Vapor-Deposited ODA-PMDA Poly(amic acid),” *Macromolecules* **37**, 5923 (2004).

M. Anthamatten, S. A. Letts, K. Day, R. Cook. A. P. Geis, T. P. Hamilton, and W. K. Nonidez. “Solid-State Amidization and Imidization Reactions in Vapor-Deposited Poly(amic acid),” *J. Poly. Sci. Part A: Polym. Chem.* **42**, 5999 (2004).

The following are LLNL internal documents:

S. Buckley and E. Fearon, "Manual - Polyamic Acid Vapor Deposition Coaters, May, 2004, UCRL-TM-206550

S. Letts, S. Buckley, and E. Fearon, "Manual - Polyimide Shell Vapor Smoothing Apparatus, August, 2004, UCRL-TM-207339

R. Sanner and R. Cook, "Recrystallization of PMDA and Synthesis of an Acetylenic Diamine," September 20, 2004, UCRL-TR-206860

**Distribution:**

Peter Amendt L-031
Paul Armstrong L-477
Tom Bernat L-481
Don Bittner L-481
Debbie Callahan L-015
Rip Collins L-481
Bob Cook L-481
Tom Dittrich L-023
John Edwards L-021
Gail Glendinning L-021
Janelle Gunther L-474
Steve Haan L-023
Bruce Hammel L-481
Steve Hatchett L-016
Denise Hinkel L-038
Nobuhiko Izumi L-399
Bob Kauffman L-466
Jeff Koch L-481
Bernie Kozioziemski L-472
Nino Landen L-473
Steve Letts L-474
John Lindl L-637
Rich London L-030
Marty Marinak L-023
Rand McEachern L-481
Mike McElfresh L-481
John Moody L-481
Dave Munro L-023
Steve Pollaine L-030
Jorge Sanchez L-481
Jim Sater L-481
Larry Suter L-031
Bob Turner L-479
Charlie Verdon L-030
Russell Wallace L-481

Mitch Anthamatten LLE
Philippe Baclet CEA
Mike Campbell GA
Jason Cooley LANL
Dave Harding LLE
Joe Kilkenny GA
Barry McQuillan GA
Abbas Nikroo GA
Art Nobile LANL
Diana Schroen SNL
Dave Steinman GA
Richard Stephens GA
Masaru Takagi GA
Marc Theobald CEA
Doug Wilson LANL